**CZECH TECHNICAL UNIVERSTIY**

**Faculty of Electrical Engineering**
**Electro-magnetic field department**

# Visible Light Communication in Case of Non Light of Sight

Diploma thesis

Study program: Communication, Multimedia and Electronics
Thesis supervisor: Prof. Ing. Stanislav Zvanovec Ph.D.,

**Bc. Dávid Novotný**

**Prague 2017**

ČESKÉ VYSOKÉ UČENÍ TECHNICKÉ V PRAZE

# ZADÁNÍ DIPLOMOVÉ PRÁCE

## I. OSOBNÍ A STUDIJNÍ ÚDAJE

Příjmení: **Novotný** Jméno: **Dávid** Osobní číslo: **434528**

Fakulta/ústav: **Fakulta elektrotechnická**

Zadávající katedra/ústav:

Studijní program: **Komunikace, multimédia a elektronika**

Studijní obor: **Bezdrátové komunikace**

## II. ÚDAJE K DIPLOMOVÉ PRÁCI

Název diplomové práce:

**Komunikace ve viditelném světle v oblastech zastínění**

Název diplomové práce anglicky:

**Visible Light Communication in Case of Non Light of Sight**

Pokyny pro vypracování:

Analyzujte využití komunikace ve viditelné části elektromagnetického spektra (Visible Light Communications, VLC) využívajících LED jak k osvětlení, tak i ke komunikačním účelům. Zaměřte se zejména na parametry příjmu v oblastech zastínění (NLOS - Non Line-of-Sight) vlivem pohybujících se osob ve vnitřních prostorách. Analyzujte statistiky příjmu a pokrytí v různých prostředích.

Seznam doporučené literatury:

[1] Ghassemlooy, Z., Popoola, W. and Rajbhandari, S., Optical wireless communications. Boca Raton, FL: Taylor & Francis, 2012.

[2] Jungnickel, V.; Pohl, V.; Nonnig, S.; Von Helmolt, C., "A physical model of the wireless infrared communication channel," Selected Areas in Communications, IEEE Journal on , vol.20, no.3, pp.631,640, Apr 2002

Jméno a pracoviště vedoucí(ho) diplomové práce:

**prof. Ing. Stanislav Zvánovec Ph.D., katedra elektromagnetického pole FEL**

Jméno a pracoviště druhé(ho) vedoucí(ho) nebo konzultanta(ky) diplomové práce:

**Ing. Petr Chvojka, katedra elektromagnetického pole FEL**

Datum zadání diplomové práce: **20.09.2016** Termín odevzdání diplomové práce: **09.01.2017**

Platnost zadání diplomové práce: **08.01.2018**

Podpis vedoucí(ho) práce | Podpis vedoucí(hó) ústavu/katedry | Podpis děkana(ky)

## III. PŘEVZETÍ ZADÁNÍ

Diplomant bere na vědomí, že je povinen vypracovat diplomovou práci samostatně, bez cizí pomoci, s výjimkou poskytnutých konzultací. Seznam použité literatury, jiných pramenů a jmen konzultantů je třeba uvést v diplomové práci.

Datum převzetí zadání | Podpis studenta

## ABSTRACT

Title: Visible light communication in case of non-light of sight

Key words: Visible light communication, Non Light-of-sight,

This diploma thesis provides analysis for communication in non-light of sight. The goal is to analyze the possibility of use the visible part of electromagnetic spectrum (Visible Light Communication, VLC) to both, communication purposes as well as illumination purposes. This diploma thesis provides different simulation scenario to investigate channel condition in case of shadowing caused by people. Simulation in matlab for this cases is provided.

## ABSTRAKT

Názov: Komunikácia vo viditeľnom svelte v oblasti zatienenia

Kľúčové slová: Komunikácia vo viditeľnom svelte, Oblasť zatienenia

Táto diplomová práca poskytuje analýzu pre komunikáciu v oblasti zatienienia. Kľúčom je analýza využitia viditeľnej časti elektromagnetického spektra pre komunikačné účely a zároveň aj k účelom bežného osvetlenia. Práca sa zameriava predovšetkým na podmienky v oblasti zatienenia spôsobené pohybmi osôb. V simulačnom prostredí matlab sú simulované rôzne scenáre komunikácie.

**Declaration**

I declare that I have prepared the master thesis without illegal help on my own only with advices of my supervisor. I also declare that contributions of other authors which are used in the thesis or led to the ideas behind the thesis are properly referenced in written form.

---

In Prague
9.1.2017

Dávid Novotný
Signature

# CONTENT


Content ..... 0

List of figures ..... 2

List of tables ..... 2

Abbreviations ..... 3

1 Introduction ..... 4

2 Optical Wireless Communication ..... 5

2.1 Visible Light Communication ..... 5

2.2 Comparison between VLC and RF communication systems ..... 6

2.3 Optical Transmitter ..... 7

2.3.1 LED structure ..... 9

2.3.2 Planar LED ..... 9

2.3.3 Edge-emitting LED ..... 9

2.4 Optical receiver ..... 11

2.4.1 Photodetector ..... 11

2.4.2 Photodetection techniques ..... 11

2.5 Modulation techniques ..... 12

2.5.1 Pulse position modulation ..... 12

2.5.2 Pulse interval modulation ..... 13

2.5.3 Pulse width modulation ..... 14

2.5.4 Modulation schemes used for diming and transmission ..... 14

3 Channel ..... 15

3.1 Line of sigth (LOS) ..... 16

3.2 Non – line of sight (N-LOS) ..... 18

3.3 Frequency selectivity ..... 19

3.4 Shadowing cause by people ..... 21

4 Simulation ..... 22

4.1 Source on the sidewall ..... 22

4.2 Source on the ceiling ..... 30
4.3 Corridor ..... 35
4.4 Movement simulation ..... 37
4.5 Summary ..... 41
5 Conclusion ..... 43
6 Reference ..... 44

# LIST OF FIGURES


Figure 1 - Frequency/Wavelenght spectrum ..... 5
Figure 2 - Typical optical link diagram ..... 6
Figure 3 - Emission spectrum of white phosphor based LED ..... 8
Figure 4 - Emission spectrum of the tri-chromatic based LED ..... 9
Figure 5 - Example of planar and Edge-emitting LED structure [2] ..... 10
Figure 6 - Lambertian pattern ..... 10
Figure 7 - Time waveforms for OOK, 16-PPM ..... 13
Figure 8 - Mapping of source data to transmitted symbols ..... 13
Figure 9 - PWM waveform ..... 14
Figure 10 - LOS & N-LOS scenario ..... 15
Figure 11 - Propagation model for difused link a)Source on the ceiling b)Source at the sidewall ..... 16
Figure 12 - CIR for channel with one source published in [2] ..... 19
Figure 13 - Different types of reflection from the wall ..... 20
Figure 14 - Spectral reflectance for different materials ..... 21
Figure 15 - 3D model of simulation 4.1 ..... 23
Figure 16 – Received power distribution simulation 4.1 1a),b),c) – obstacle → [0.4 ; 0.4; -1] ..... 24
Figure 17 – Propagation delay simulation 4.1 1a),b),c) – obstacle → [0.4 ; 0.4; -1] ..... 26
Figure 18 - Received power distribution simulation 4.1 2a),b),c) – source → [0 ; 2; 2] ..... 27
Figure 19 - Propagation delay simulation 3.1 2a),b),c) – source → [0 ; 2; 2] ..... 29
Figure 20 - Received power distribution simulation 4.2, obstacle [0.4 ; -0.8; -1] ..... 31
Figure 21 – Propagation delay simulation 4.2, obstacle [0.4 ; -0.8; -1] ..... 31
Figure 22 - Channel Impulse Response simulation 4.2 – freq. selective surface ..... 32
Figure 23 - Received power distribution simulation 4.2, obstacle [0.4 ; -0.8; -1], Room size 5x5x3 ..... 33
Figure 24 - CDF for Room 4x4x3 and 5x5x3 ..... 33
Figure 25 – Propagation delay simulation 4.2, obstacle [0.4 ; -0.8; -1] , Room size 5x5x3 ..... 34
Figure 26 - Channel Impulse Response simulation 4.2 – freq. selective surface, Room size 5x5x3 ..... 35
Figure 27 - Received power distribution simulation 4.3 obstacle [-0.5 ; -0.5; -1.5] ..... 36
Figure 28 – Propagation delay → simulation 4.3 obstacle [-0.5; -0.5; -1.5] ..... 37
Figure 29 - CDF for simulation 4.3 with one source and 2 sources ..... 37
Figure 30 - RMS delay spread ..... 38
Figure 31 - mean delay spread ..... 39
Figure 32 - Transmission speed Rb, Received power Rc, mean delay ..... 40
Figure 33 - mean delay dependend on FOV / Receiver height ..... 40
Figure 34 - Received power dependend on FOV / Receiver height ..... 41


# LIST OF TABLES


Table 1 RF/VLC Comparrison ..... 7
Table 2 - Simulation parameters for square based Room ..... 22
Table 3 - Source and Obstacle positions for 4.1 ..... 23
Table 4 - Parameters for simulation 4.2 ..... 30
Table 5 – Exponential distribution for reflected signal strength loss ..... 34
Table 6 - parameters for simulation 4.3 ..... 35
Table 7 - parameters for simulation 4.4 ..... 38

# ABBREVIATIONS

| | |
|---|---|
| ADP | Avalanche photodiode |
| CIR | Channel impulse response |
| CIR | Chanel impulse response |
| D2D | Device to device communication |
| E-L | Electric to light |
| IM-DD | Intensity modulation/direct detection |
| IR | Infra-red |
| LAN | Local area network |
| LD | Laser diode |
| L-E | Light to electric |
| LED | Light emitting diode |
| LOS | Line-of-sight |
| MIMO | Multiple-input Multiple-output |
| M-PAM | Multi-level pulse amplitude modulation |
| M-PPM | Multi-level pulse position modulation |
| N-LOS | Non line-of-sight |
| NRZ | Non-return to zero |
| OOK | On-off keying |
| OWC | Optical wireless communication |
| PWM | Pulse width modulation |
| RF | Radio frequency |
| RGB | Red, Green, Blue |
| VLC | Visible light communication |

# 1 INTRODUCTION

This diploma thesis is focused on the visible light communication. Analysis of using the possibility to use LED sources to illumination, as well as for communication puproses with use of suitable modulation will be provided in next pages. LED diodes are becoming more affordable than ever and their popularity increases. Different situations will be simulated in simulation environment matlab, to provide results and follow up analysis.

Simulation will be oriented to NLOS – Non Line-of-Sight communication in indoor environment. The most popular technology used in indoor environment those days is Wi-fi. So the comparison of basic differences between communication using visible light and the radio frequency wawes would be appropriate.

In the simulation, different types of room and different receiver position will be taken look at. Theoretical backround for simulation will be provided in the next pages to acquire distribution of electromagnetic field, propagation delay or changeable channel statistics caused by person movement.

Also interesting, should be to consider how the different types of material will effect the NLOS communication and compare simulation results for the frequency selective and frequency non-selective approach.

# 2 Optical Wireless Communication

Communication is essential factor in human history. Communication witnessed an enormous transformation in last few decades, especially electronic commucation has witnessed huge research and development. Demand for high-quality service is increasing as the need for higher bandwidth. To meet the demand for short-range interchange links, optical wireless communication (OWC) can be used.

OWC is an innovative technology that offers flexible networking solutions. There are many advantages like license-free wireless broadband connectivity in the contrast to radio frequency RF connections. Since the infrared (IR), ultraviolet (UV) or visible light can be used to carry the signal huge license free spectrum of approximately 670 THz is available [1]. Netwrok solutions based on OWC also provide cost-effective, highly secure high-speed connectivity for a number of applications such as video, voice, data, illumination an many others [2]. As the mobile devices are about to rule the category of consumer devices, demand for reliable technologies supporting the mobility of user increases. As the mobile devices are often relatively small, the usable area for the receiver is not huge.

## 2.1 Visible Light Communication

Visible light is used to carry the information in the visible light communication (VLC) systems. Figure 1 shows the frequency/wavelength spectrum. Unlike IR or UV the VLC systems are not used only for data interchange but also for an illumination to kill the two birds with one stone.

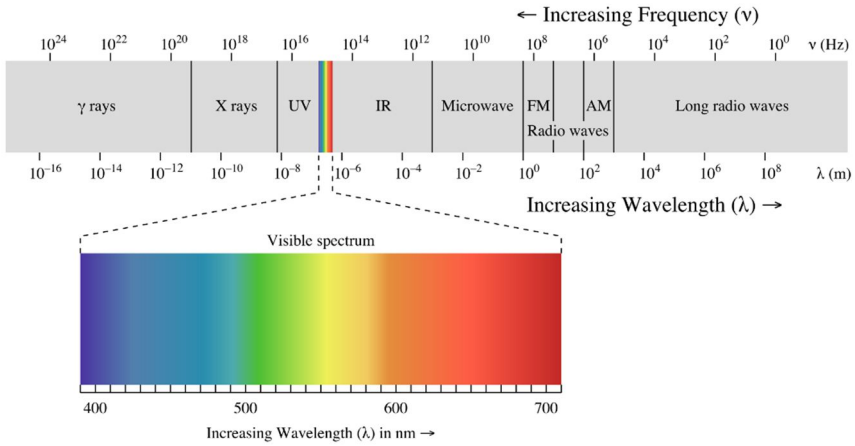


*Figure 1 - Frequency/Wavelenght spectrum*

Increased popularity of solid-state lightning caused growing research in VLC in last few years. LEDs has longer lifetime compared to other artificial light sources like incandescent

light bulbs or others. Figure 2 shows example of typical optical link diagram, block channel coding takes care of getting input signal to binary form, modulation block provides desired modulation scheme to the signal. E-L circuit, for conversion of electric signal into ligh, and visible light source block can be think of as one block and outcome from this block is information coded into visible light. VLC is a wireless communication so the channel medium is (mostly) air. At the receiver side, photodiode/photodetctor block converts light back into electrical form, this electrical signal is demodulated in the demodulation block and finaly decoded.

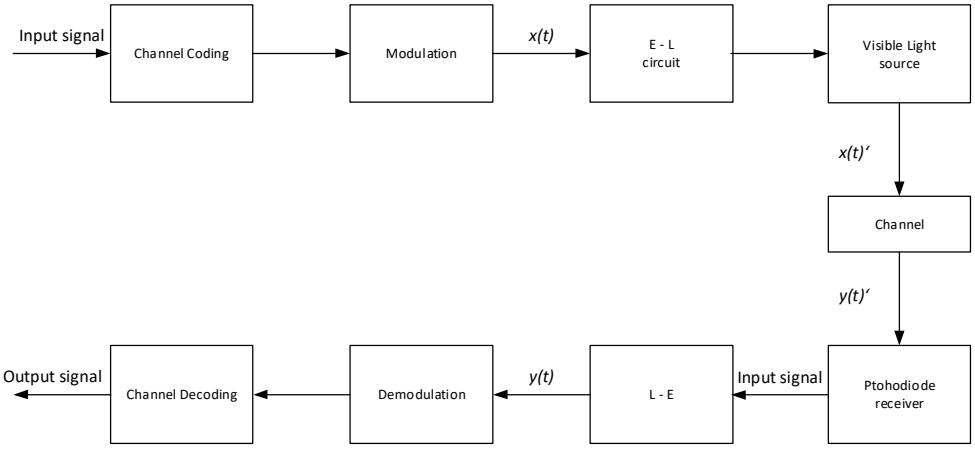


*Figure 2 - Typical optical link diagram*

The visible light represents no harm for human eye as the LED is used as light source unlike the IR LEDs. Highly efficient white LEDs combine the prime colours: red, green and blue. Communication systems based on VLC offer a several advantages but on the other hand, there are also challenges that need to be addressed. Not only the LED has to offer high luminous intensity, but the good color quality as well, LEDs must be able to switch off and off very rapidly [2,20].

## 2.2 Comparison between VLC and RF communication systems

RF communication systems are often used for short-range wireless links. The RF wireless local area networks LANs uses license free spectrum at 2.4GHz, 5.7GHz and the proposed at 17 GHz and 60 GHz. Recently, the Wireless Gigabit Alliance has proposed the utilization of the mm-waves in the license-free 60 GHz band. In this high frequency 7GHz bandwidth is available and that enables 7 Gbps short-range wireless links. The same band, 60 GHz has been also considered as a part of the IEEE 802.11 ad framework, 802.11ad is meant to high data speed links in wireless local area networks (WLANs) with use of multiple-input multiple-output (MIMO) techniques [6]. In contrast, VLC systems covering

unlicensed spectral range of cca 400-700 nm [7]. Both communication systems are short-range links because they suffer for a high path loss.

RF channels are more robust to blocking and shadowing due to the diffraction and scattering of RF wawes. On the other hand VLC channel is much more susceptible to shadowing/blocking, thus the light emitted from a light source can not penetrate through the walls so the communication is contained within the room unlike the RF communication [2, 6]. Since the the light can not pass through solid objects like walls, it is easy to sustain the communication within the room, thus the communications utilizing this type of transmission can provide higher security.

When it comes to deploying a new technology in real life scenario one of the most important element is price. The LEDs used as light source and the photodiode used for recevieving the optical singal are fairly cheap and available (LEDs are already used in cars, buses, traffic lights, white LEDs are repleacing the light bulbs in offices/homes) [2, 8]. Led are not affected by the catastrophic degradation mechanism in general, which can severely affect injection lasers [25]. Table 1 RF/VLC Comparrison provides the basic comparison betwen RF and VLC systems.

*Table 1 RF/VLC Comparrison*

| Characteristic | OWC | RF |
|---|---|---|
| Regulated bandwidth | No | Yes |
| Pass through solid objects | No | Yes |
| Multipath dispersion | Yes | Yes |
| Coverage range | Short | Short |
| Path loss | High | High |
| Dominant noise | Backround | Other RF users |

## 2.3 Optical Transmitter

Generally, there are many light sources, but only a certain group of them could be used as optical transmitter in the OWC. The mostly used light sources in OWC are laser diodes (LD) and light-emitting diodes LEDs. Laser diodes produce coherent light (highly direction beam) and thus are mostly used for outdoor applications. LEDs produce incoherent light, several nanometers wide spectrum and are used for indoor application.

In the VLC should light source serve not only as data transmitter but also fro illumination, so in order to meet this requirement white LEDs are needfull. Invention of efficient blue LEDs

prepared the way for energy saving white light source devices, so the VLC technology is able to take advantage of the infrastructure based on white LEDs [9].

Efficient blue LEDs are giving rise to two different types of technology to manufacture white LEDs, the first type is phosphor based LEDs and the other is tri-chromatic based LEDs. The emission spectrum of each white LED, phosphor based and tri-chromatic based LED was measured in the visible range in [10]. Figure 3 and Figure 4 are adopted from [10] and shows emission spectrum of two white LEDs type.

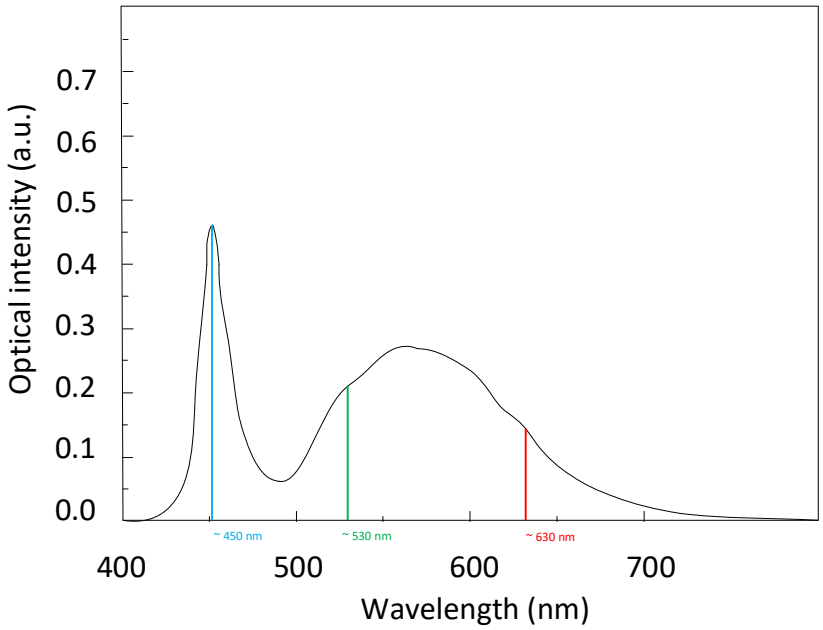


*Figure 3 - Emission spectrum of white phosphor based LED*

In Figure 3 is shown emission spectrum of phosphor based LED, as apparent the spectrum consist of sharp strong peak at ~ 450 nm (blue light) and the broad emission at ~ 500 – 650 nm (red light ~ 630 nm, green light ~ 530 nm), this broad emission is achieved by the short wavelength absorption from the blue LED by the fluorescent phosphor layer. Note, that individual wavelengths which corresponds with 3 basic colors are highlighted in Figure 3 and Figure 4 with its matching color. This layer absorbs part of the blue light and re-emits the light of a longer wavelength. In human perception, the white light is visible. Tri-chromatic RGB white LED has, in comparison to the phosphor based LED, 3 distant peaks, as apparent from Figure 4 that match RGB color wavelength.

Emission from optical source is termed as Lambertian when the LEDs emits light from all surfaces. The optical power radiated from a unit area into a solid angle in the Lambertian emission is constant (surface irradiance is when power isn't radiated from unit area into a unit angle). Maximum intensity of radiated optical power in Lambertian radiaton, $I_o$, is to the LED

surface perpendicular. On the sides $I_o$ reduces wit cosinus of viewing angle as expressed in equation (1) [2].

$$I_o(\theta) = I_0 * \cos(\theta) \quad (2)$$

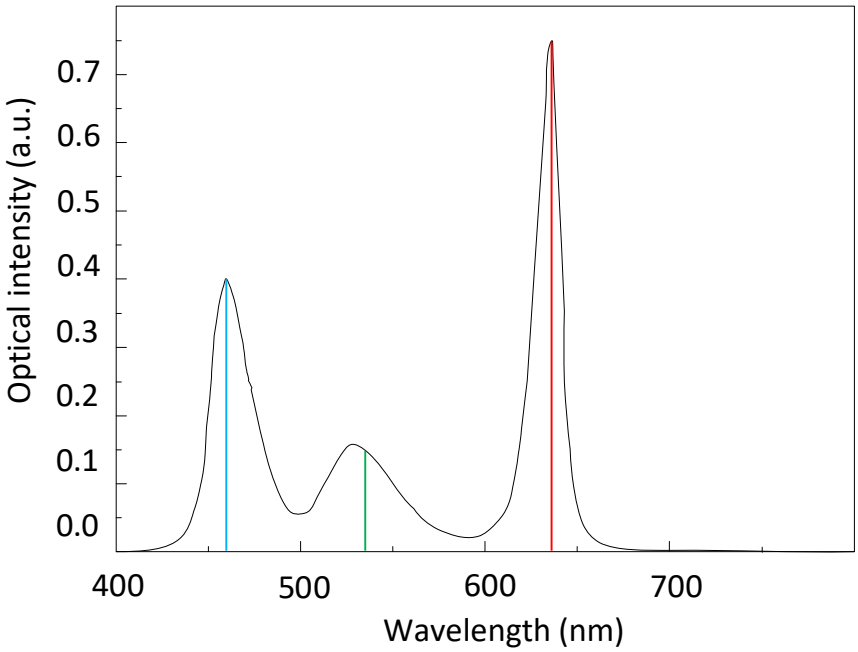


*Figure 4 - Emission spectrum of the tri-chromatic based LED*

### 2.3.1 LED structure

LEDs are solid state light emitting devices that are more efficient than classic light sources, this means they radiate less heat and thus their lifespan is longer. Structure of an LED is a p-n junction and wavelength of emitted light is given by extrinsic material type. The wavelength peak depends on the band-gap energy of the p-n junction, this is depended on semiconductor material making the junction [1,3,22].

### 2.3.2 Planar LED

Structure of an LED can be complex, but the simplest LED structure can be found at planar LED. Planar LEDs structure is fabricated by either vapour or liquid epitaxial process over the whole surface [23]. As mentioned above, when the LED emits light from all of its surfaces then the emission can be expressed as Lambertian. This is the case for planar LEDs, therefore planar LEDs are termed as Labmertian. Lambertian pattern is shown in Figure 6.

### 2.3.3 Edge-emitting LED

When the light emitted into all directions is not desirable, thus omnidirectional planar LEDs are not fit to meet this requirement for emiting , edge-emitting LEDs are way to go. To achieve this edge-emitting LEDs confining the light in a thin (50 – 100 μm) narrow stripe

in the plane of the p-n junction [24,8]. Edge-emitting LEDs are more complex and more directional than planar LEDs.

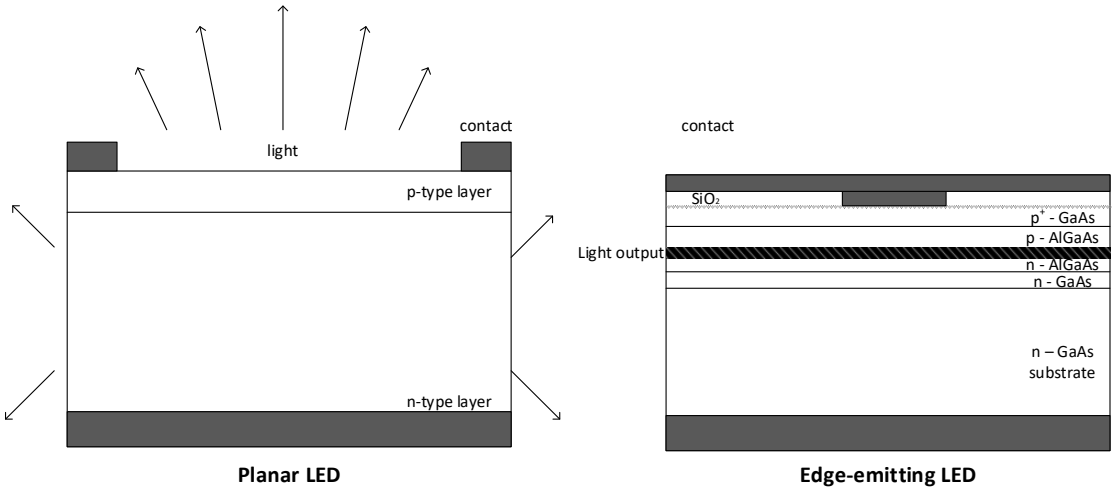


*Figure 5 - Example of planar and Edge-emitting LED structure [2]*

Figure 5 shows example of planar LED emittin on all surfaces and tructure of a double hetero-junction AlGaAs edge-emitting LED.

Figure 6 - Lambertian patternshows normalized Lambertian characteristics, where $\theta$ is semi-angle (in some papers referd as $\theta_{1/2}$ ) at half power and the $m_1$ expressing source beam directivity (Lambert's mode number) (3).

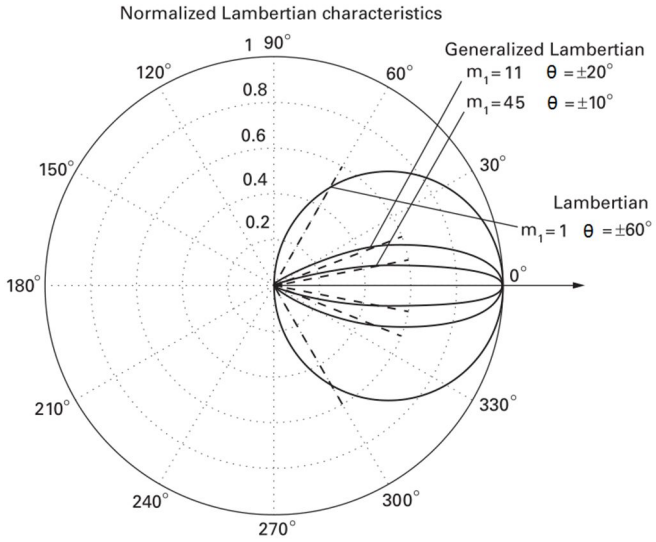


*Figure 6 - Lambertian pattern*

## 2.4 Optical receiver

Communication is process of exchanging the information between the source and the receiver. In VLC systems the receiver has to be able receive information in form of light sent from the transmitter. When it comes to the size of the receiver, larger receiver detector area would provide better signal to noise ratio but at a cost of increased capacitance (this would have a limited effect on transmission capacity due to limiting the receiver bandwidth). Next factor is receiver use in the mobile devices, as the number of mobile devices is rapidly increasing, thus small area is available [1, 14].

### 2.4.1 Photodetector

The photodetector is a solid-state converter that converts optical signal into electrical form. Converteted signal is proportional to the square of instantaneous optical flow and converted signal is proportional to the instantaneous received power. The photodector must meet the requirements for high sensitivity in operational wavelength window, adequate bandwidth for the desired data rate, thermal stability and since the optical signal is in general very weak, low noise level is needed. LED sources has a long life, therefore the same characteristic for the long lifespan and low cost is called for from photodetctors. Photodetector material composition determines its operation wavelength window. For example, the silicon pin photodiode has operating wavelength (300-1100 nm), germanium pin photodiode (500-1800) [2,12].

PIN photodector contain a very lightly n-doped intrinsic region between semiconductor p-type, n-type materials. PIN photodector is able to convert photon into electric current if the energy of incoming photon is larger than band-gap energy of semiconductor material [25]. Another is type of photodector is ADP photodector. ADP photodector varies from the PIN photodector in area of providing an inherent current gain through repeated electron ionization process. This process results in increased sensitivity since the photocurrent is multiplied before the thermal noise caused by the receiver circuit is encountered.

### 2.4.2 Photodetection techniques

The process of converting information carried by the light is called photodection. As mentioned above, photodetctor converts optical signal into equivalent electrical singal, so the information could be decoded on the receiver side. Mostly in OWC there are two different detection schemes. Intensity modulation/direct detection (IM-DD) and coherent detection schemes. IM-DD is widely used because of its simplicity, IM-DD scheme offers a advantage, because the receiver sensitivity is independent of the incoming signal state

of polarization and the carrier phase, which can randomly fluctuate. Coherent detection is more complex but offers ability to restore amplitude and the phase component [13, 14].

Direct detection – this method detects only intensity of light that is being emitted from the optical source. Transmited information is associated with the intensity variation of transmitted electromagnetic field for the receiver to recover the original information encoded in to the optical signal. Instantaneous photodetector current *i(t)* is given by: [14]

$$i(t) = \frac{\eta_{qe} q \lambda}{hc} MP(t) \qquad (4)$$

Where *h* is a Planck constant, *c* is speed of light, $\lambda$ is wavelength, *P(t)* is instantaneous incident power, *M* is a photodector gain factor, *q* is electronic charge $\eta_{qe}$ is a quantum efficiency.

Coherent detection – Information is encoded by using amplitude, frequency and the phase of the optical signal. Receivered signal at the receiver side is combined with optical local oscillator. The frequency of optical local oscillator may vary from the from the frequency used for carrying the information [15]. Benefits of this detection method are redeemed by receiver sensitivity to the phase and state of polarization, so coherent systems are much more complicated than systems using IM-DD photodetection technique [2,13].

## 2.5 Modulation techniques

The LEDs has two purposes in VLC systems, serve as light source for illuminiation and at the same time for communication role. To achieve this, the dimming part and the communication part must not interfere with each other. In the other words they must be independent. Few modulation techniques to meet this requirements will be introduced in the following lines.

### 2.5.1 Pulse position modulation

In VLC systems, where the light source produces incoherent light, the data transmission is realized through intensity modulation and direct detection (IM/DD) (due to its simplicity and also low cost) , so the transmitted signal between the source and the receiver needs to be real-valued and non-negative. In order to achieve this, single carrier modulation technique such as multi-level pulse position modulation (M-PPM) and multi-level pulse amplitude modulation (M-PAM) is used. In optical wireless system the signal modulates the intensity of the optical emitter, and therefore it needs to be real-valued and unipolar non-negative [1, 2].

PPM modulation technique is used in applications with average power limitations. This modulation is an orthogonal modulation and improves the power efficiency off on-off

keying (OOK), but the drawback is greater complexity and increased bandwidth requirement [3].

Figure 7 shows that An L-PPM symbol consists of a constant power pulse occupying one slot duration within L (where $L=2^M$ and M indicates available total states number) possible time slots and others time slots are empty [1,3].

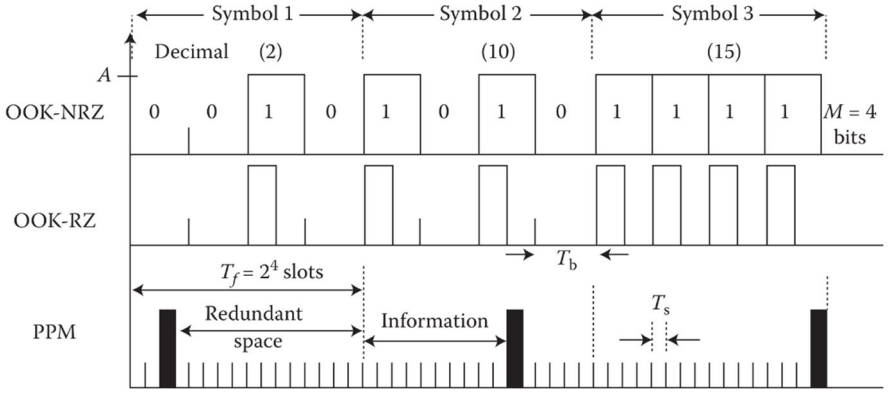


*Figure 7 - Time waveforms for OOK, 16-PPM*

### 2.5.2 Pulse interval modulation

Pulse interval modulation (PIM) reduces the complexity of PPM modulation. Information is encoded by number of empty slots inserted between two pulses. DPIM brings better performance by removing redundant space in comparison to PPM modulation. As shown in Figure 8, DPIM is an modulation technique that is asynchronous. This means that each block of M (where $M=\log_2 L$) input data bits $\{d_i, i = 1, 2, \ldots, M\}$ is mapped to one of $L$ possible symbols $\{s(n), 0 < n < L\}$ of different length. Whit DPIM being isochronous modulation, the number of empty slots is fully dependent on the decimal value of the $M$-bit data stream being endoced. Synchronization is secured due to the pulse always being at the start of the symbol [2, 4].

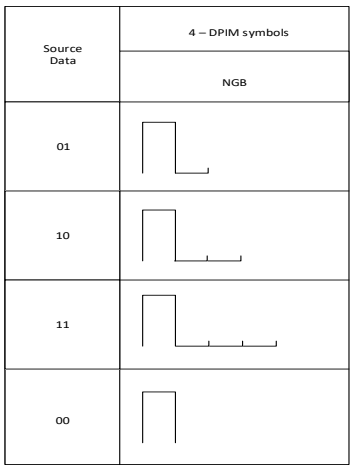


*Figure 8 - Mapping of source data to transmitted symbols*

### 2.5.3 Pulse width modulation

As apparent from the modulation name, pulse width modulation (PWM) use different pulse width to encode the information. This fact enables wide range of brightness level (0-100%) by controlling modulation index and the pulse duration is used to control the LED drive current. Because in VLC, the LED is used for illumination, it is important that this modulation technique is undetectable for the human eye. In order to achieve this, the diming frequency is typicaly above 100 Hz [5]. Leading or trailing edge of a square wave is used to achieve the brightness change with no effect on light emitted color. The duration of *k*-th symbol is given as:

$$\tau_k = \tau_0\left[1 + M_{pwm} m(kT_c)\right] \quad (5)$$

Where $\tau_0$ is unmodulated pulse width representing $M_{pwm}m(kT_c) = 0$, and $M_{pwm} = 2\Delta\tau/T_c$ is the modulation index ($0 < M_{pwm} < 1$), $\Delta\tau$ is the peak modulated time, $T_c$ is the sampling interval and *m(t)* is the input signal. In Figure 9 is shown an example of PWM modulation [2, 5].

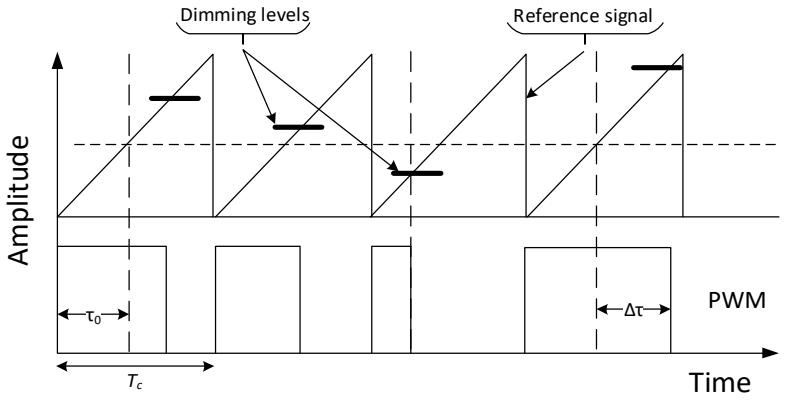


*Figure 9 - PWM waveform*

### 2.5.4 Modulation schemes used for diming and transmission

The IM/DD is most preferred method of signal transmission, consequently the modulation techniques with on-off keying – non-return to zero (OOK-NRZ) are mostly used [9,19]. Pulse modulation schemes based on PWM dimining schemes does not suffer from the wavelength shift due to current variation in the intensity/amplitude modulation diming mechanism [18]. So the PWM can solve the dimming, to achieve the combination of dimming and data transmission, the PWM is traditionaly used combined with the PAM modulation [17]. As an alternative method to PWM combined with PAM, overlapping PPM, which has been suggested in [21] and meets the requirement for both illumination and data transmission when the channel conditions are invariable, can be used [22].

# 3 CHANNEL

Understanding the characteristics of the channel is essential, so an optical communication systems could be designed. Signal attenuation is in the majority caused by two factors, the optical path loss and multipath dispersion. In a directed LOS channel scenario, reflections do not need to be taken into consideration. Thus in this circumstances only path loss is easily calculated from knowledge of distance between source and receiver, receiver size and the transmitter beam divergence.

Due to reflections on different walls or obstacles in a non-LOS scenario we have to ponder with multiple paths that optical signal can get from the source to the receiver. Thus the path loss prediction is more complex. In Figure 10 is shown difference between LOS and N-LOS optical link.

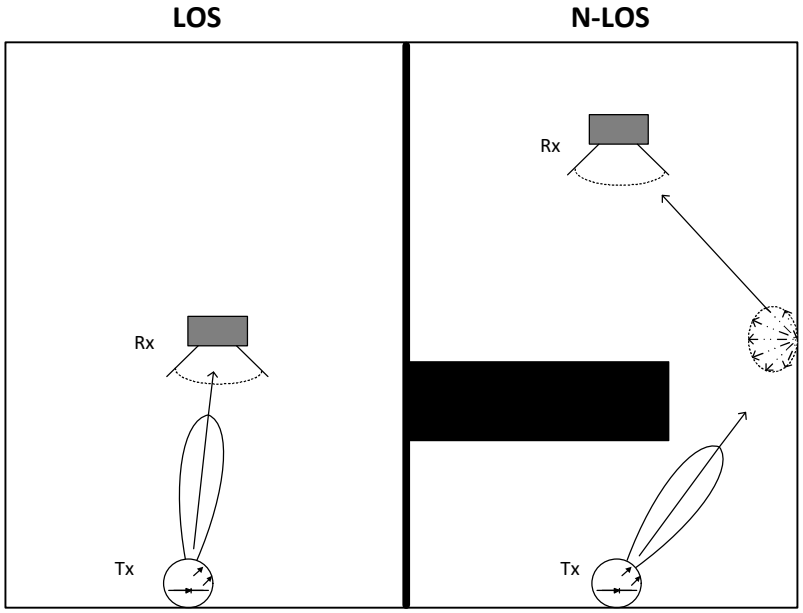


*Figure 10 - LOS & N-LOS scenario*

In LOS link, the dominant component of received power is received power from the source via the direct link. Power reflected from the walls is more attenuated due to higer distance the light has to travel from the LED transmitter to the photodetector, but also reflection causes received signal to decrease even more (because of certain reflectivity index and diffuse reflection). The reflections are modelled as Lambertian and reflection coefficient is discussed further. Propagation delay varies in case of LOS and NLOS link. In LOS scenario, predictably, delay for direct path is less than in the case of reflected path. In NLOS scenario, there is no direct visibility available, only propagation delay caused by reflected signal is present.

As the source is placed at the sidewall, it is important to realize that reflection from the wall opposite to the source is analogous to the reflection from the floor in case of source being on the ceiling.

The reflection, from the floor for the case shown in Figure 11 a), is not considered in most simulation, due to usually smaller floor reflectivity index $\rho$ ($\rho$ is material dependent) and the fact that photodector is facing upwards (usually FOV is no more than 90°, so reflected signal from the area located beneath the receiver can't reach the photodector area). In case, as is represented in Figure 11 b) - source at the sidewall, the opposite wall reflection differs from the one from the sidewalls (relative to the position of the transmitter), the DC gain from opposite wall is higher, because angles $\alpha_{ir}$, $\beta_{ir}$ are smaller (thus the cosine value is higher), so the $H_{ref}(0)$ (13) is expected to be higher.

## 3.1 Line of sigth (LOS)

In LOS optical link, shown in Figure 1, there is direct visibility between source and receiver. Since the distances in indoor OWC are not significant, the attenuation caused by scattering and absorption is very low.

Visible light communication systems uses as a source an LED. Figure 11 shows a propagation models of diffused link considered in simulation. Situation with the source on the ceiling a) is a typical situation, where the light source position at the sidewall b) could represent a device to device communication (D2D).

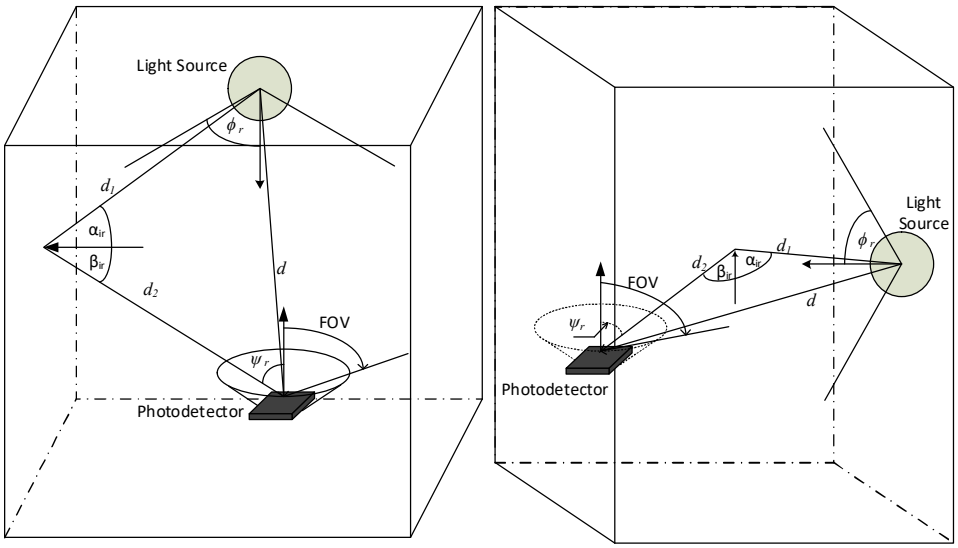


*Figure 11 - Propagation model for difused link a)Source on the ceiling b)Source at the sidewall*

Generalized Lambertian radiant is used for modelling of the radiation intensity pattern [2]:

$$R_0(\phi) = \begin{cases} \frac{m_1+1}{2\pi}\cos^{m_1}\phi & for\ (\Phi\ \in [-\frac{\pi}{2},\frac{\pi}{2}] \\ 0 & for\ \phi\ \geq \frac{\pi}{2} \end{cases} \quad (6)$$

$m_1$ expressing source beam directivity (Lambert's mode number). $\Phi$ = 0 is the angle of maximum radiated power. The order of Lambertian emission $m_1$ is

$$m_1 = \frac{-\ln 2}{\ln\left(\Phi_{\frac{1}{2}}\right)} \quad (7)$$

$\Phi_{1/2}$ is LED semiangle at half-power. The total received power at the receiver is given by

$$P_r = P_t H_d(0) \quad (8)$$

Where $H_d(0)$ is DC gain of the direct path, $P_t$ is optical power that is transmitted by LEDs. Where $H_d(0)$ is given as

$$H_d(0) = \begin{cases} \frac{(m_1+1)}{2\pi d^2} A_{det}\cos^{m_1}(\phi_r) T_s(\vartheta) g(\vartheta) cos(\vartheta) & 0 \leq \vartheta \leq \vartheta_{FOV} \\ 0 & \vartheta > \vartheta_{FOV} \end{cases} \quad (9)$$

In short-distance links, multipath dispersion presents only a minor problem. Since we can ignore multipath dispersion. LOS links channel models assume the LOS path dominates and the LOS links are modelled as a linear delay and attenuation. Impulse response can be expressed as [2]

$$h_{los}(t) = \frac{A_r(m_1+1)}{2\pi d^2}\cos^{m_1}\phi\, T_s(\Psi) g(\Psi)\cos\Psi\, \delta\left(t - \frac{d}{c}\right) \quad (10)$$

$c$ is the speed of light, $\delta$ is the Dirac function and $\delta$ $(t - d/c)$ is the signal propagation delay, $g(\Psi)$ is optical gain of an ideal nonimaging concentrator, $Ts(\Psi)$ – optical filter gain. Direct path between transmitter and the receiver is in LOS scenario always available and there is no obstacle that could cast a shadow that would have an impact on direct visibility. Also no spatial alignment between pattern of detection on the side of the receiver and on the transmitter radiation pattern.

Chanel impulse response (CIR) is only single peak, because only a direct path is considered. Propagation delay is proportional to time the light needs to travel the distance between the source and the receiver.

## 3.2 Non – line of sight (N-LOS)

While directed LOS links provide high irradiation intensity at the receiver and a wide channel coherence bandwidth, they are not suitable for scenarios where high user mobility is required, and the link can be easily interrupted or blocked.

As mentioned above, for the LOS links that are non-directed and diffuse links, path loss is more complex to predict. Altogether the optical path loss depends on several factors like objects in the room, the walls, ceiling reflectivity, shape and size of the room. In general the received power at photodetector $P_r$ can be expressed as

$$P_r = P_t H_d(0) + \int P_t H_{ref}(0) \tag{11}$$

Unlike LOS links also reflected signal is considered. $P_t$ is total transitted power by optical source. $H_{ref}(0)$ stands for DC gain on reflected path and can be expressed as [2]

$$H_{ref}(0) = \begin{cases} \dfrac{A_r(m+1)}{2(\pi d_1 d_2)} \rho \, dA_{wall} \cos^{m_l}(\phi_r) \cos(\alpha_{ir}) \\ \times \cos(\beta_{ir}) \, T_s(\Psi) g(\Psi) \cos(\Psi_r) \qquad 0 \le \Psi_r \le \Psi_c \\ 0 \qquad\qquad\qquad\qquad\qquad\qquad elsewhere \; \Psi_r > \Psi_c \end{cases} \tag{12}$$

Where *d1* and *d2* are distances between reflective point and LED, and between a receiver surface and a reflective point, *m* expresses the Lambert index of LED light source, $dA_{wall}$ is a reflective area of small region, $\rho$ is the reflectance factor, $\phi_r$ is the angle of irradiance to a reflective point, $\psi_r$ is the angle of incidence from the reflective surface, $\alpha_{ir}$ , $\beta_{ir}$ are the angles of incidence to a reflective point and the angle of irradiance from the reflective point to the receiver.

Total received power can be calculated by using (9), although due to multipath character of the optical link, the delay profile of the channel need to be described. The mean excess delay $\mu$ is defined by [2]

$$\mu = \frac{\sum_{i=1}^{M} P_{d,i} \, t_{d,i} + \sum_{j=1}^{N} P_{ref,j} \, t_{ref,j}}{P_r} \tag{13}$$

Where $P_{d,i}$ is received optical power from *i*-th direct path and the $P_{ref,j}$ is optical power received from *j*-th reflected path. The RMS delay spread present critical upper bound criterion of data transmission rate. RMS delay spread is given by [2]

$$D_{RMS} = \sqrt{\mu^2 - (\mu)^2} \tag{14}$$

And $\mu^2$ is defined by

$$\mu^2 = \frac{\sum_{i=1}^{M} P_{d,i} \, t_{d,i}^2 + \sum_{j=1}^{N} P_{ref,j} \, t_{ref,j}^2}{Pr} \tag{15}$$

Impulse response of the channel is dependent on various factors as receiver and source position, type of material used to cover the walls, thus spectral reflectance for specific wavelength and room size. Figure 12 shows how to simulation result of channel impulse response (CIR) could look like, it was published and adopted from [2]. Simulated room size is 2.5 x 2.5 x 3 and the source is placed on the ceiling. First reflection from the sidewalls is considered. On the left part is also LOS link visualized, on the right side only N-LOS link is available.

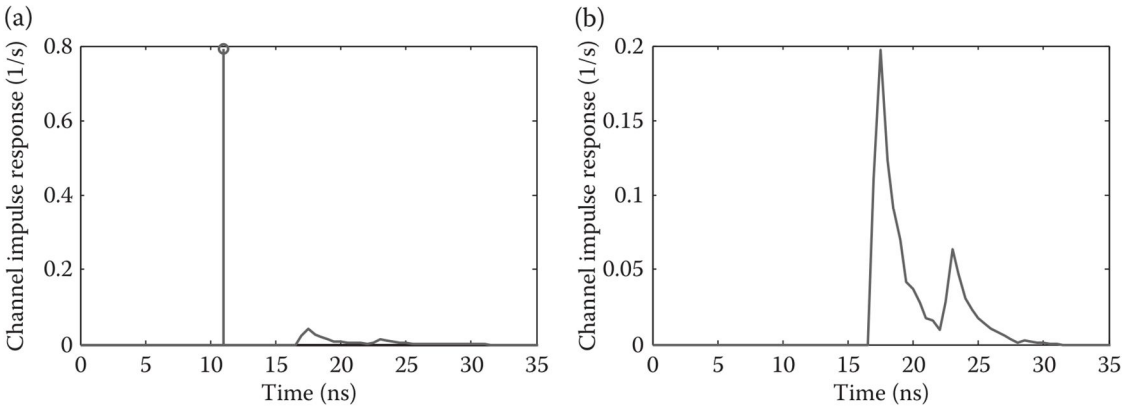


*Figure 12 - CIR for channel with one source published in [2]*

Maximum achievable data rate in diffuse channel, can be calculated from (14) this data rate can be transmitted through the channel with no need for an equalizer [2]

$$R_b \leq \frac{1}{10 * D_{RMS}} \tag{16}$$

And the channel bandwidth can be expressed as

$$BW \leq \frac{1}{\Delta T} \tag{17}$$

Where $\Delta T$ describes the delay between the LOS signal and the onset of the diffuse signal.

## 3.3 Frequency selectivity

The optical N-LOS links in VLC systems can be consider to be non-frequency selective to reduce complexity of simulation. Light radiated from white LEDs is being composed from 3 basic colors (red, green, blue) as shown in Figure 3 or Figure 4. The reflection characteristics may vary for particular wavelength, it is dependend on several factors including, not only particular wavelength, but also the surface material, angle of incidence $\theta_{LED}$ or the surface roughness relative to the wavelength.

Rayleigh criterion is mostly adopted to determine the texture of a surface. According to this criterion, a surface can be considered smooth if the maximum height of the surface irregularities conforms to the following [2, 7]:

$$h_{si} < \frac{\lambda}{8 \sinh(\theta_i)} \tag{18}$$

So the wall reflectivity depends not only on wavelength but material used in the wall as well. Although specular reflections can occur from a mirror or other shiny object, most of the reflections are typically diffuse in nature, and mostly they are well modelled as Lambertian [1, 2]. In Figure 13 are shown types of reflection that can occur. Later in the simulation only difuse reflections from the wall are assumed.

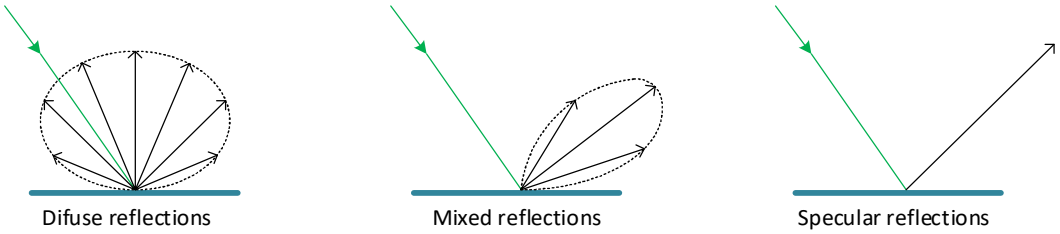


*Figure 13 - Different types of reflection from the wall*

Figure 14 shows how can reflectance be different for different wavelength but also for different textures. Spectral reflectance was measured for plaster, plastic wall, ceiling and for the floor.

Individual wavelengths that correspond with 3 basic colors are highlighted with its matching color in the figure for a plaster wall, estimated spectral reflectance for each color is is for blue color (around 450 nm) ρ = 0.65, for green color (around 530 nm) ρ = 0.75 and for the red color (around 630 nm) ρ = 0.82. Figure 14 is adopted from [11]. Spectral reflectance for each color is later used in frequency selective simulation.

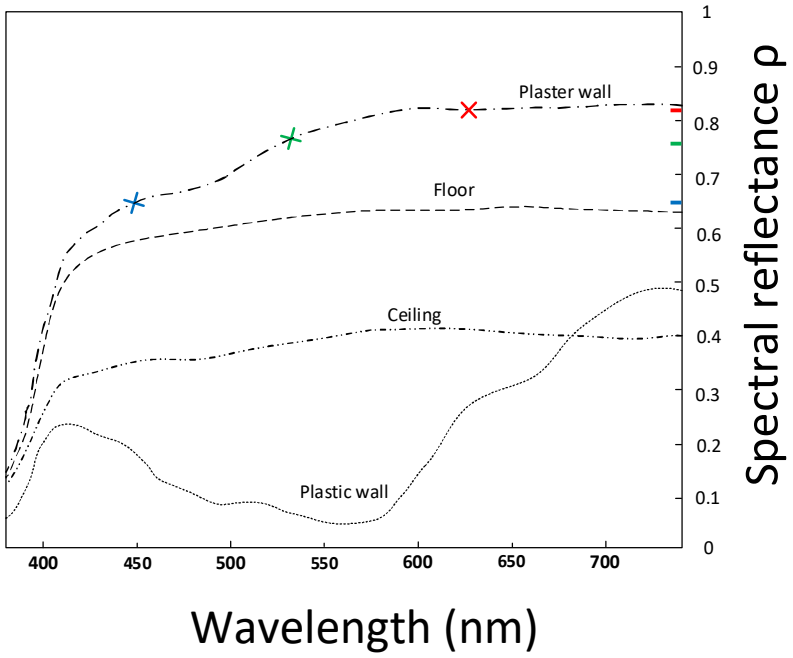


*Figure 14 - Spectral reflectance for different materials*

## 3.4 Shadowing cause by people

To investigate the impact caused by a moving person to the chanell characteristics in indoor environment, human body needs represent with corresponded model. Dimensions of human body model are 0.5 x 0.25 x 1.8 m.

Movement of people was selected to cover various obscuring situations. The source is placed in the middle of the room on the ceiling and because the room shape is symmetrical (and due to source in the midlle results would be reciprocal), movement is simulated only in ¼ of the room (bottom right side).

The mobility is simulated in discrete steps, user is turned back to source and the receiver is in his hands (the consequence, a human body is shadowing the direct path from the source to the receiver, this result in only NLOS link communication available).

In every simulation steps, all parameters are calculated in the position where the receiver is. In the simulation is considered not only shadowing of LOS link, but also shadowing of NLOS link caused by obstacle → obstacle is blocking some paths for reflected signal either from the wall or even on its way to the wall. To cover more scenario, the receiver will be simulated in different height and that is 1m, 1.2m and 1.4m.

# 4 SIMULATION

In the simulation the VLC system is single-source based. These single-source systems are tending to suffer more from signal blocking than multiple-sources systems, on the other hand the multiple-sources system will suffer more from intersymbol interference due to multipath propagation [2]. Only direct path and first reflection is considered. The second order reflection contributes less than 1dB to total received power and the computation time would be significantly longer. Shadowing caused by people is investigated, human being is represented by black box with proportions stated in Table 2 as well as simulation parameters for 4.1 and 4.2. Note that in Table 2 number of LED in array and the transmitted power by LED are stated. To calculate total power transmitted by source $P_t$

$$P_t = P_{per\ LED} * number\ of\ LED \tag{19}$$

*Table 2 - Simulation parameters for square based Room*

| | |
|---|---|
| Room size | 4m X 4m X 3m |
| Detector area | 0.01 $m^2$ |
| Transmitted power by LED - $P_{per\ LED}$ | 0.01 W |
| Number of LED | 100 |
| Reflection coefficient ρ | 0.8 |
| Transmitter position [x,y,z] a) | Simulation dependent X 2m X 2m |
| Transmitter position [x,y,z] b) | 0 X 0 X 3m (on the ceiling) |
| Receiver height | 1 m |
| Semi-angle at half power θ | 70° |
| FOV of the receiver | 90° |
| Obstacle proportions [x,y,z] | 0.5m X 0.25m X 1.8m |

## 4.1 Source on the sidewall

At first the source is placed on the sidewall and radiate optical power into the room, so the maximum radiated power is in horizontal plane. For better visualisation 3D model is shown in Figure 15. Only first reflection from west, south and east wall is simulated. Since the source is placed on the north wall, there are only secondary (and higher) reflections from the north wall, thus no first order reflection is present.

Table 3 displays different positions of source 1a), 1b), 1c) (black box si placed on the ground at [x=0.4 ; y=0.4 ; z=-1.5] ) and obstacle positions 2a), 2b), 2c) (source placed at [x=0 ; y=2 ; z=2] ).

*Table 3 - Source and Obstacle positions for 4.1*

| 4.1 Source on the sidewall | a) | b) | c) |
|---|---|---|---|
| 1) Source position [x ; y ; z] | [-1 ; 2 ; 1.5] | [0 ; 2 ; 1.5] | [1 ; 2 ; 1.5] |
| 2) Obstacle position [x ; y ; z] | [-1.5 ; 1 ; -1] | [ 1 ; 0 ; -1] | [0.3 ; -0.9 ; -1] |

3D model shows simulation assumption that signal is reflected from sidewalls (west, east wall) and opposite wall (south wall - relative to source position placed on the north wall). LOS link is not available in the shadowed area due to blocking by obstacle. Note that no reflection from ceiling or floor is taken into consideration.

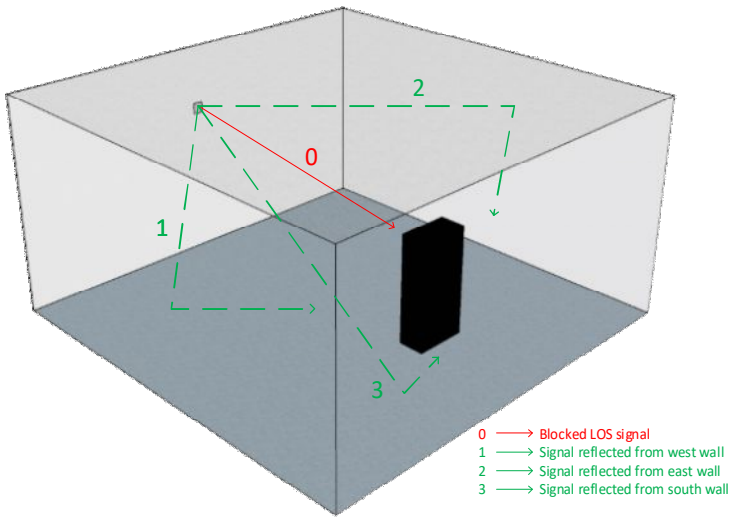


*Figure 15 - 3D model of simulation 4.1*

In the first part of simulation 4.1 different transitter position are simulated, the receiver is in height of 1m. Number of discrete steps in grid attributable for 1m is 8. Received power distribution is calculated in every grid postion. In the second part of simulation 4.1 different positions of obstacle (person) are simulated. The white rectangle in simulation results, represents where the model of human being is situated.

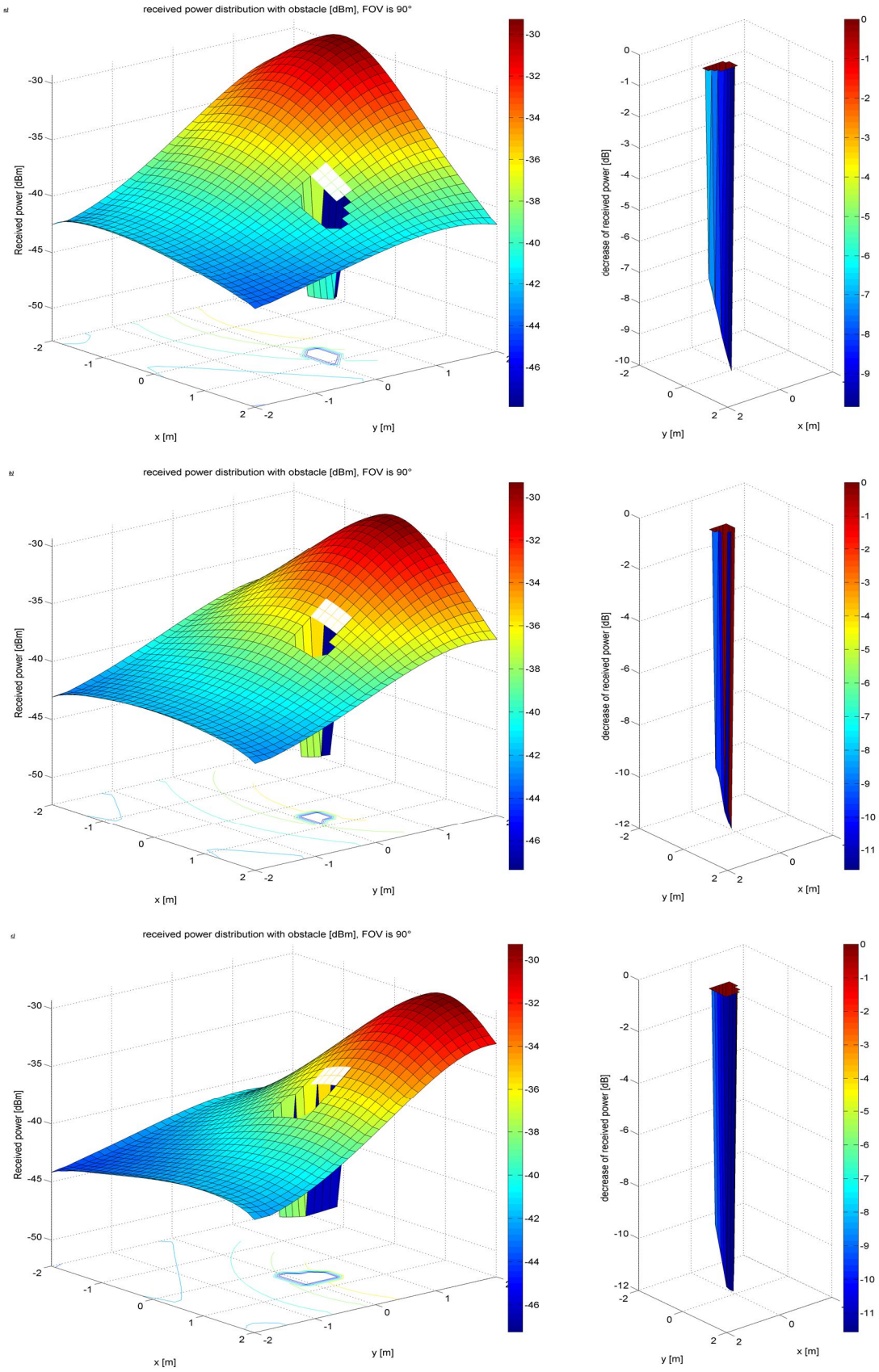


*Figure 16 – Received power distribution simulation 4.1 1a),b),c) – obstacle → [0.4 ; 0.4; -1]*

In Figure 16 the received power distribution is pictured for 3 different source position. Intuitevely the LED source placement can be read from the receiver power distribution (maximum of received power in x axis ) or view in Table 3. As expected significant drop of received power is visibile in the shadowed area. In this area only NLOS link is available (first reflection from the walls). For better visialisation the received power decrease (received power with object causing signal blocking substracted from empy room scenario) is shown on the figure right side. The drop is in range from cca 7dB to less than 12 dB dependend on transmitter position. Note that on the right side of figure axis are in reverse order so the drop in received power could be represent by its matching color on colorbar. The closer the object is to the source, the bigger is margin between received power from LOS link and NLOS link, thus received power reduction become more noticeable.

Figure 17 represents propagation delay for simulation 4.1. a),b),c). For each case, two subplots are shown, the first subplot with distinctive peak that has lower delay time is simulation without human being, so the direct path is present. On the other subplot subplot blockade is considered, so signal can get from the source to the receiver only via reflected path. Note that y axis is normalized to the maximum value of received signal. In case of b) and c) the reflected signal from east wall is strongest (from the reflected signal), as the signal has to travel the shorhtest distance from LED to photodector. Photodector is placed below obstacle (y coordinate is smaller). In case of b) signal reflected from west and east wall varies varies only slightly due to similar conditions.

Signal reflected from the south wall isn't weaker as we could expected in the classic simulation with the source on the ceiling, reason for this is explained in 3. In a nutshell, since the source is termed as Lambertian, emiited light in the direction towards the south wall has higher energy (Maximum intensity of radiated optical power in Lambertian radiaton, $I_o$ , is to the LED surface perpendicular). So even if the light has to travel longer way to the photoreceiver, in the end the signal can be still stronger than signal with shorther path. It is appropriate to mention that time resolution is ½ ns, therefore value of received singal from the wall can be a slightly misleading. In the case of a) the results are even less intuitive, as it may appears the longer path signal travels, the stronger it gets.

Again, reason for such a result is the placement of the source an the receiver and thus angle of α and β. For better understanding take another look at Figure 11 - Propagation model for difused link a)Source on the ceiling b)Source at the sidewall.

Simulation results for 4.1 - 2) begins on page 27.

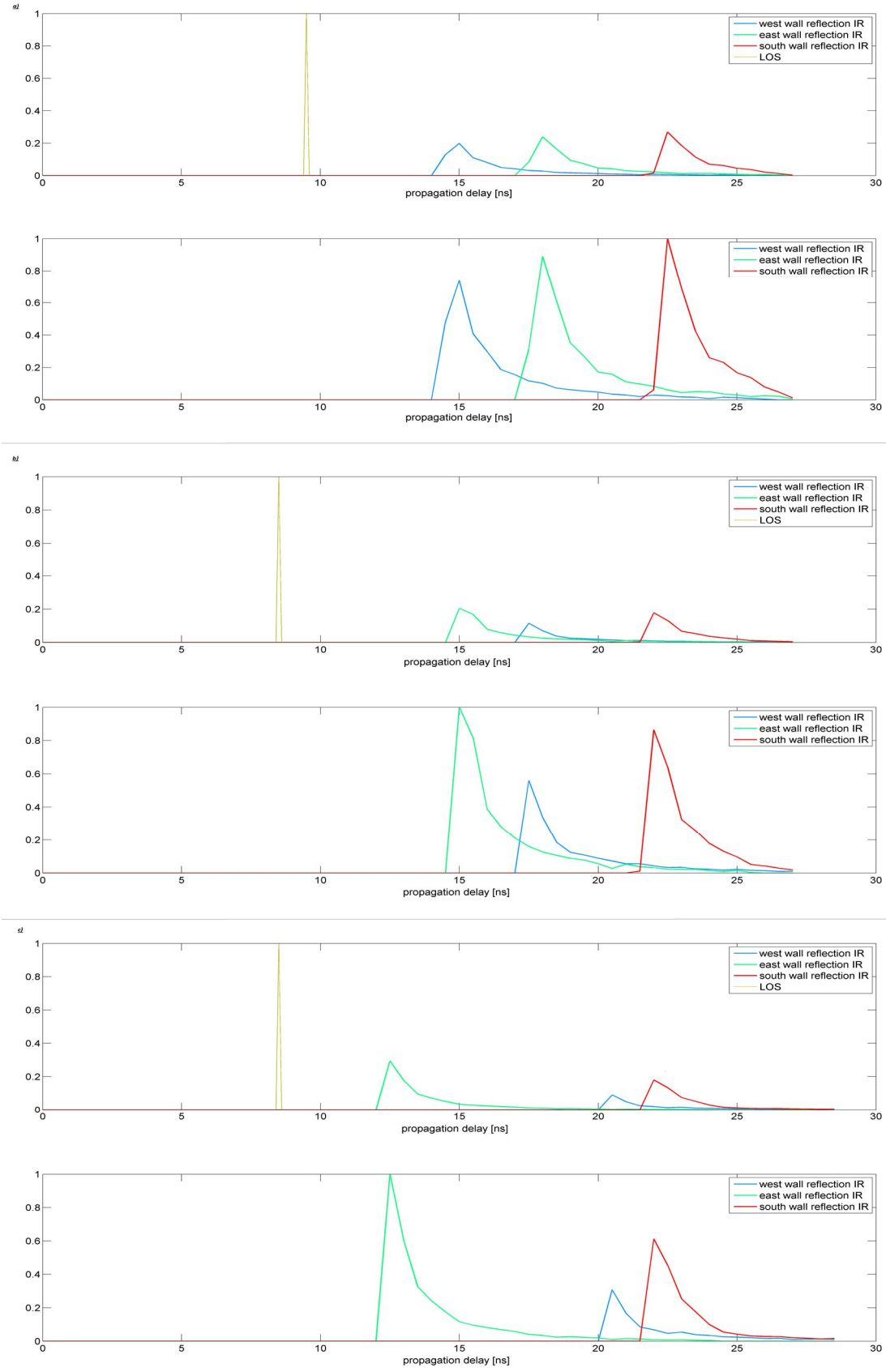


*Figure 17 – Propagation delay simulation 4.1 1a),b),c) – obstacle → [0.4 ; 0.4; -1]*

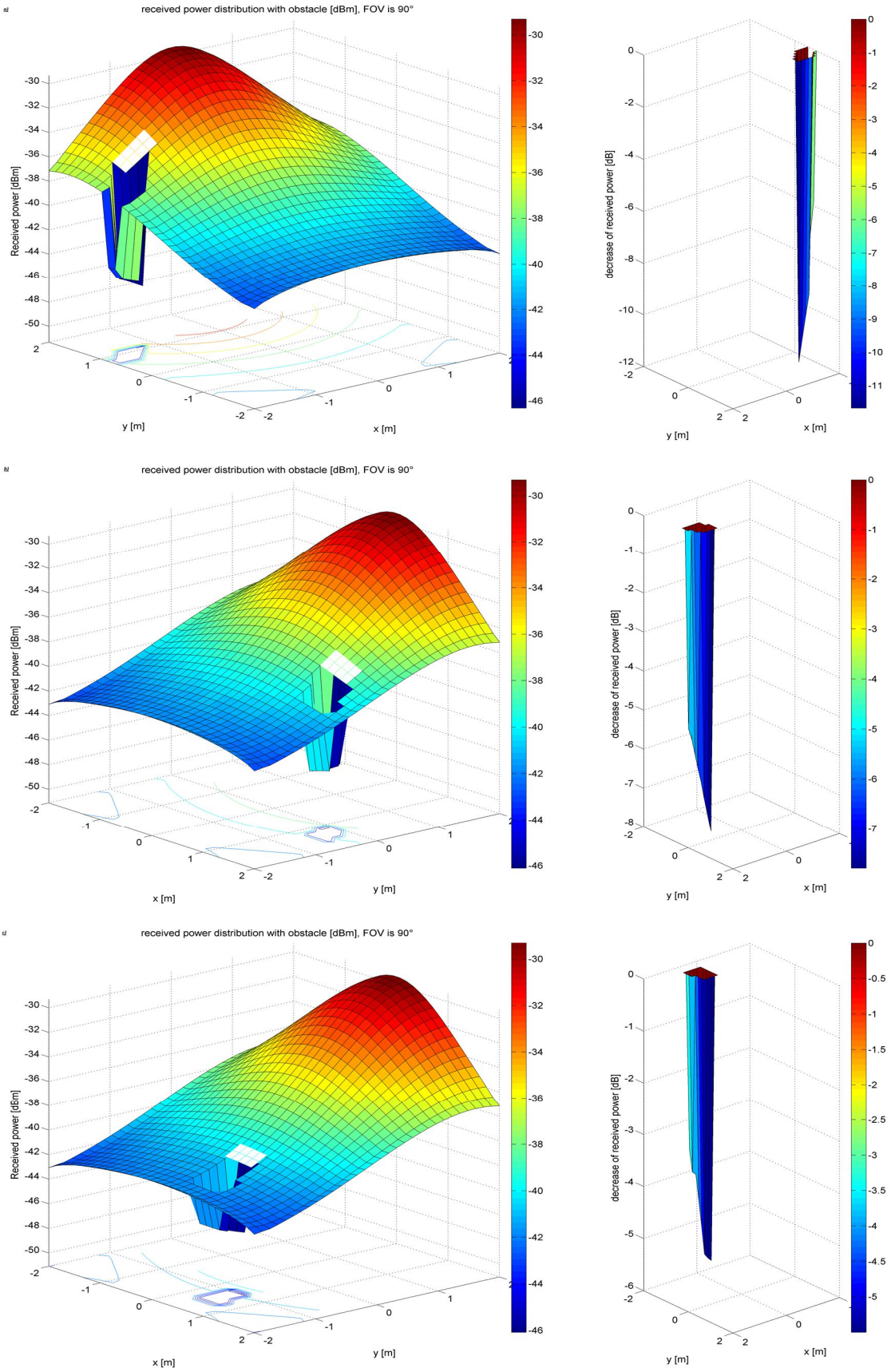


*Figure 18 - Received power distribution simulation 4.1 2a),b),c) – source → [0 ; 2; 2]*

The next scenario simulated was with static source placed at [0; 2; 2]. Component that is providing the movement in this case is modelled human being. Three different positions were chosen to study impact of human body to the VLC system displayed in Figure 18. Again note that on the right side of figure, decrease in received power is visible and for accurate color characterization (matching the colorbar value), the axis are in reverse order. Also in the first case a) the 3D view of received power distribution has different viewing angle (difference is 90° anticlockwise ) to offer a better figure projection. As mentioned before, human body distance from the source is inversely proportional to decrease in received power, due to LOS link fading. In the case where the object causing shadowing is further from LED source, the drop is only from 3 to 5 dB.

In case of a) the drop is between 6 and little more than 11 dB. Value of received power is logarithmic proportional to area of the receiver, so if the receiver are would be 10 times larger (for example receiver with are 2.5x4cm instead of 1x1cm) it would enhance the received signal by 10 dB as apparent from (20).

Figure 19 shows propagation delay for simulation 4.1 2). Position of obstacle in case of a),b),c) are in Table 3. In the case of a) the object casing shadowing is close to the west wall, thus relatively strong peak from west wall is visible as well the relatively small time spacing between the LOS signal and the signal reflected from the west wall. On the other hand, reflection from the east wall is far off in terms of amplitude (cca 10%) as well as time spacing. South wall reflection is a bit stronger than the one mentioned in previous sentence (cca 20% of the west wall amplitude [cca -7dB]).

In the case of b) the situation is a bit more similar to 4.1 1)b). About the signal reflected from the opposite wall to the receiver, can be said the same as in simulation 4.1 - 1)).

In case of c) the reflected signal is almost as strong as LOS signal. It is appropriate to underline since the value of received signal is normalized. Note also that in direct LOS link there is only one path from source to the receiver, but for reflected signal there are many paths ( for south wall ideally → X size * Z size * number of grid in 1m → if the FOV would be 180° ) from the source to the receiver.

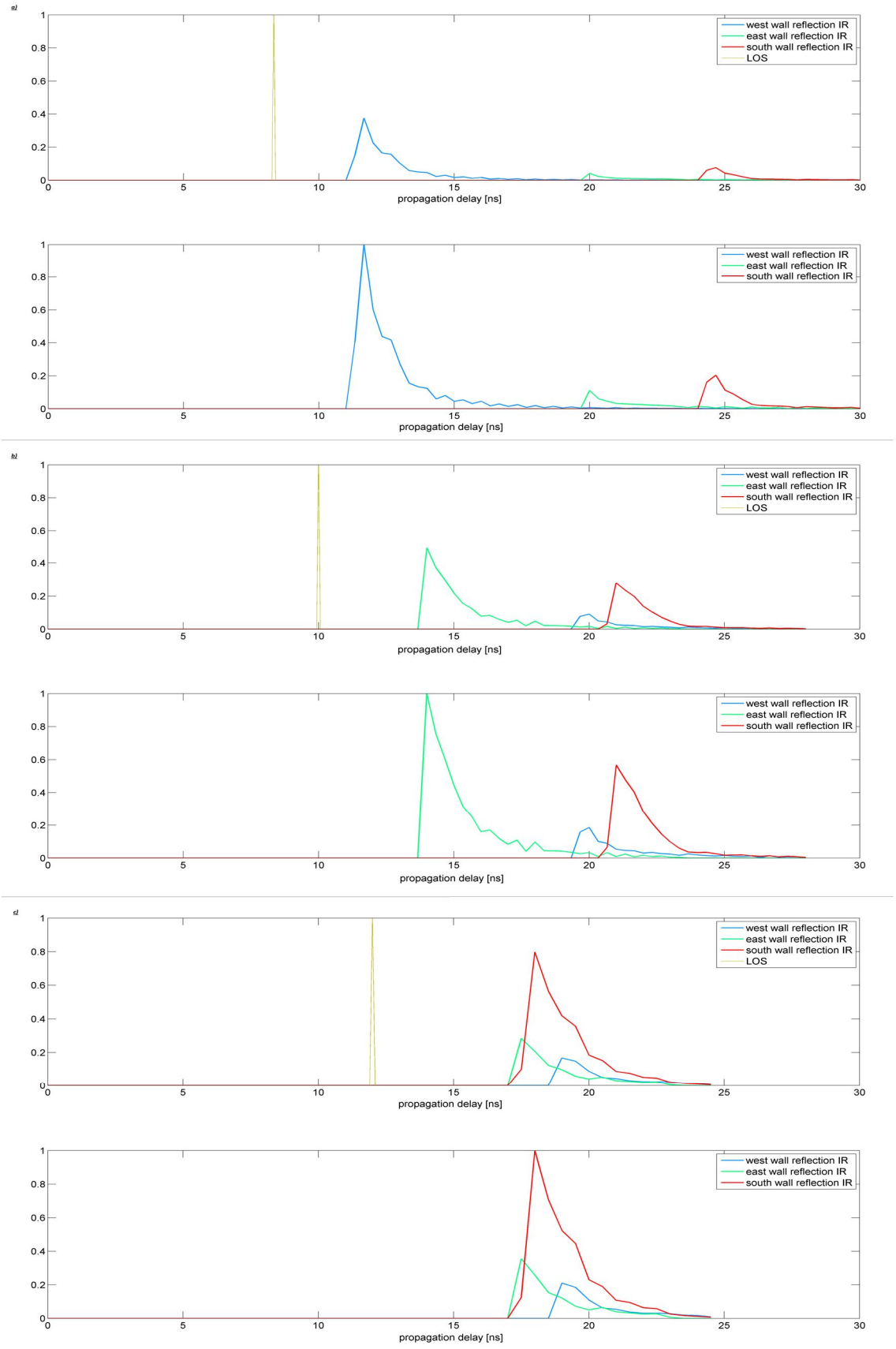


*Figure 19 - Propagation delay simulation 3.1 2a),b),c) – source → [0 ; 2; 2]*

## 4.2 Source on the ceiling

Now the source is placed in the middle of the room on the ceiling. This is a case of more conventional situation when the source is facing to the ground and thus maximum radiated power is perpendicular to the celing. To compare different room size, simulation with two different sizes will be investigated. First the room size is 4x4x3m and then we will add another meter to x and y dimension so the room size is in the second simulation 5x5x3m. Parameters for the simulation are shown in Table 4:

*Table 4 - Parameters for simulation 4.2*

| | |
|---|---|
| Room size 1st simulation<br>Room size 2nd simulation | 4m x 4m x 3m<br>5m x 5m x 3m |
| Detector area | 0.01 $m^2$ |
| Transmitted power by LED - $P_{per\ LED}$ | 0.01 W |
| Number of LED | 100 |
| Reflection coefficient ρ | 0.8 |
| $\rho_{red}$ | 0.82 |
| $\rho_{green}$ | 0.75 |
| $\rho_{blue}$ | 0.65 |
| Transmitter position [x,y,z] a) | 0 x 0 x 3m (on the ceiling) |
| Receiver height | 1 m |
| Semi-angle at half power $\theta$ | 70° |
| FOV of the receiver | 90° |
| Obstacle proportions [x,y,z] | 0.4m x -0.8m x 1.8m |

Figure 20 shows that power distribution received by the receiver is more uniform in comparison with source placed at the sidewall, especially in the room corners (for example in the south-west corener the received for LOS link is around 6dB stronger than in 4.1 1b) simulation). Shadow projected by obstacle is not so exteted asi in 4.1 simulation, due to the higher source placement. Note the x,y axis on the right side are reversed so the drop in received power could be represent by its matching color on colorbar. The decrease of received power is up to 9 dB. The value of signal drop in area with no LOS link is similar to 4.1 simulation, because the difference between LOS link and NLOS link is similar, but the total received power from LOS link or either the NLOS link is stronger due to the shorter distance between the source and the receiver, even the reflected path is shorter though. White rectangle represents the object that causes shadowing, which represents common person.

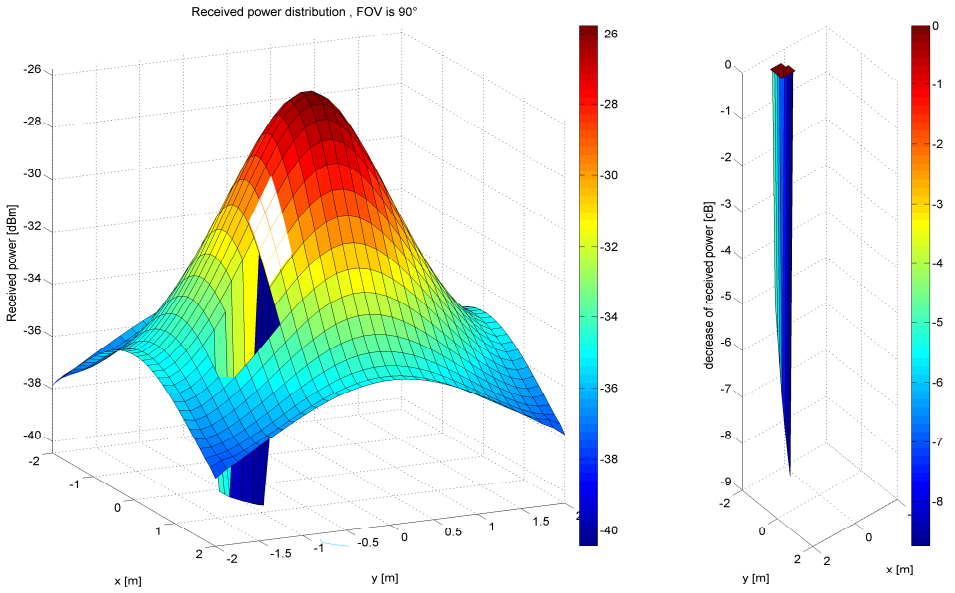


*Figure 20 - Received power distribution simulation 4.2, obstacle [0.4 ; -0.8; -1]*

Figure 21 shows Channel impulse response, time resolution is 0.5 ns. Reflection from each side is color coded for better visualization. Loss of signal strength reflected from each wall is following exponential distribution shown in subplot. Note that y axis is normalized to the maximum value of received signal.

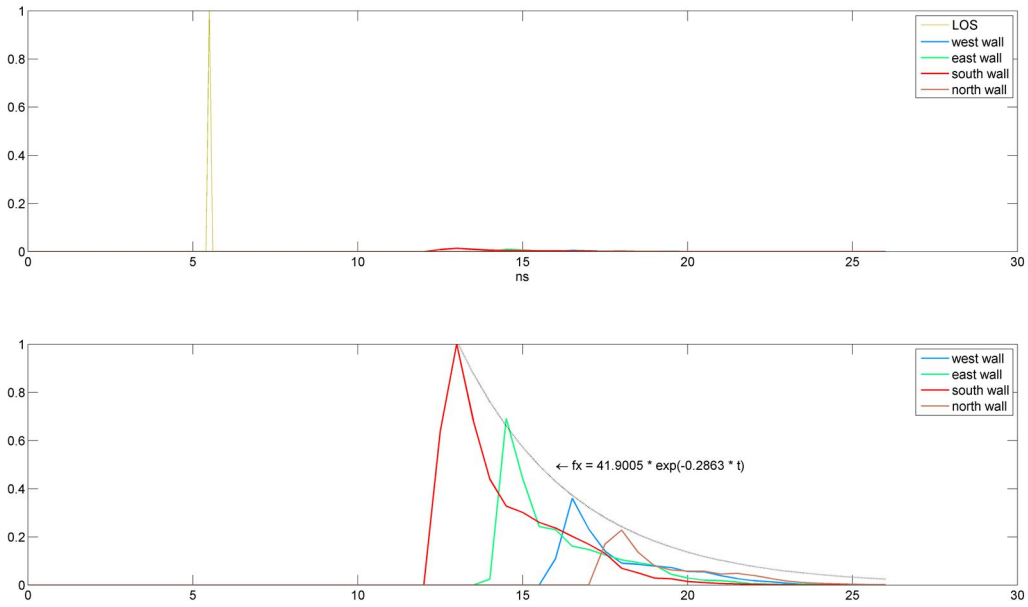


*Figure 21 – Propagation delay simulation 4.2, obstacle [0.4 ; -0.8; -1]*

Since the source is placed in short distance from the receiver, thus if there would be a LOS link available, the LOS componenet would be dominant. NLOS component shown in Figure 21 is strongly attenuated in comparison with the LOS component.

Until now, the side walls in the all previous simulations was considered to be nonfrequency selective. Providing spectral emission for two different types of LED (Figure 3 - Emission spectrum of white phosphor based LED and Figure 4 - Emission spectrum of the tri-chromatic based LED) as well as spectral reflectance for RGB colors (Figure 14), the simulation for Source on the ceiling - 4.2 was realized and the results can be seen in Figure 22. Time resolution is 0.5 ns.

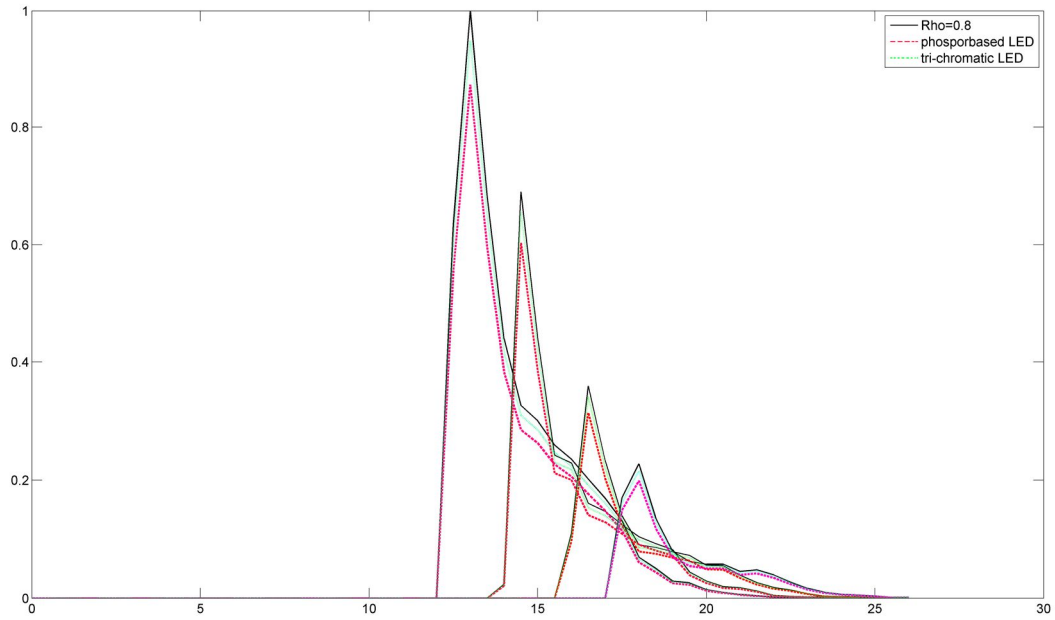


*Figure 22 - Channel Impulse Response simulation 4.2 – freq. selective surface*

The black color represents the simulation from previous Figure 21, where ρ is set to 0.8 and the walls are considered to be frequeny non selective, thus every wavelength is reflected equally. The parameters ρ for each color are shown in Table 4. Relative intensity for each color and for both LED are determined based on emission characteristics for phosphor based LED shown in Figure 3 and emission characteristics for tri-chromatic based LED displayed in Figure 4. As apparent from the Figure 22, the difference is insignificant and is possible to treat wall as frequency non-selective in this case.

Naturally, this is possible without inaccuracy when we consider wall with almost constant reflectivity index. If the reflectivity index for the wall would differ more significantly for individual wavelength, (different type of materials [26]) it would be more accurate to treat the walls as frequency selective.

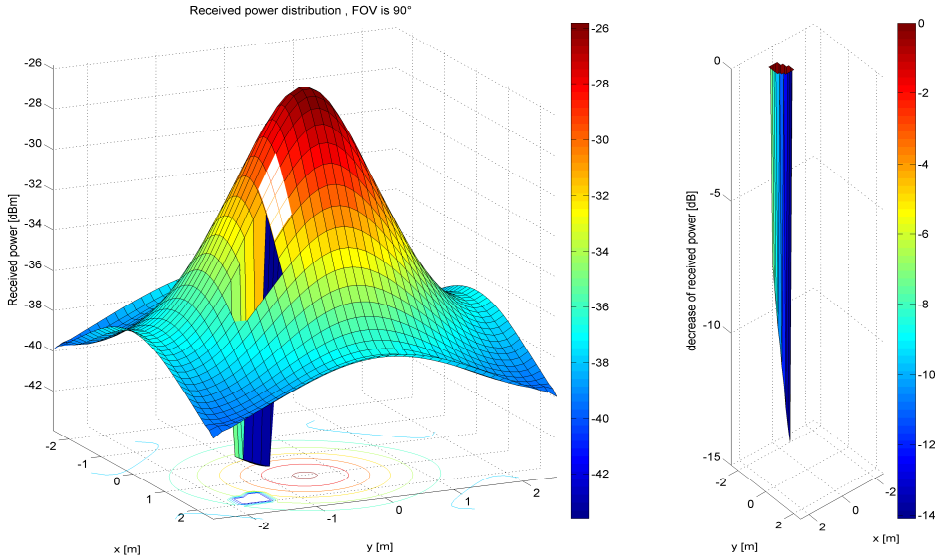


*Figure 23 - Received power distribution simulation 4.2, obstacle [0.4 ; -0.8; -1], Room size 5x5x3*

Figure 23 shows power distribution at the receiver for he room size 5x5x3. As the received power in the shadow area is dependent only on reflected signal, increasing the room size will cause more significant decrease in received power. Room resize caused the drop in received power 14dB, in comparison to less than 9dB with smaller room. To better see the impact of room dimension increase by 1m in both, x and y dimension, central distributed function CDF is shown in Figure 24.

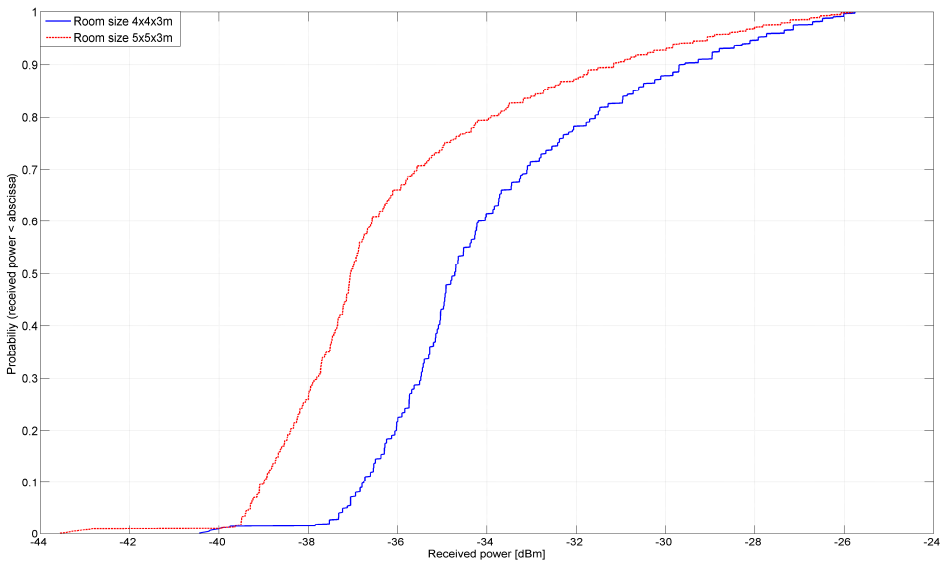


*Figure 24 - CDF for Room 4x4x3 and 5x5x3*

The LOS component in propagation delay will remain untouched since the distance between LED and photodector doesn't change (Figure 25). NLOS component will be more suppressed, reflected signal has less energy. Propagation delay of reflected signal (NLOS component) is increased by cca 3 ns, which corresponds with time the light needs

to travel 1 m. Keep in mind room expansion by 1m effectively means expansion on both sides by 0.5 m. Time resolution for propagation delay is 0.5 ns.

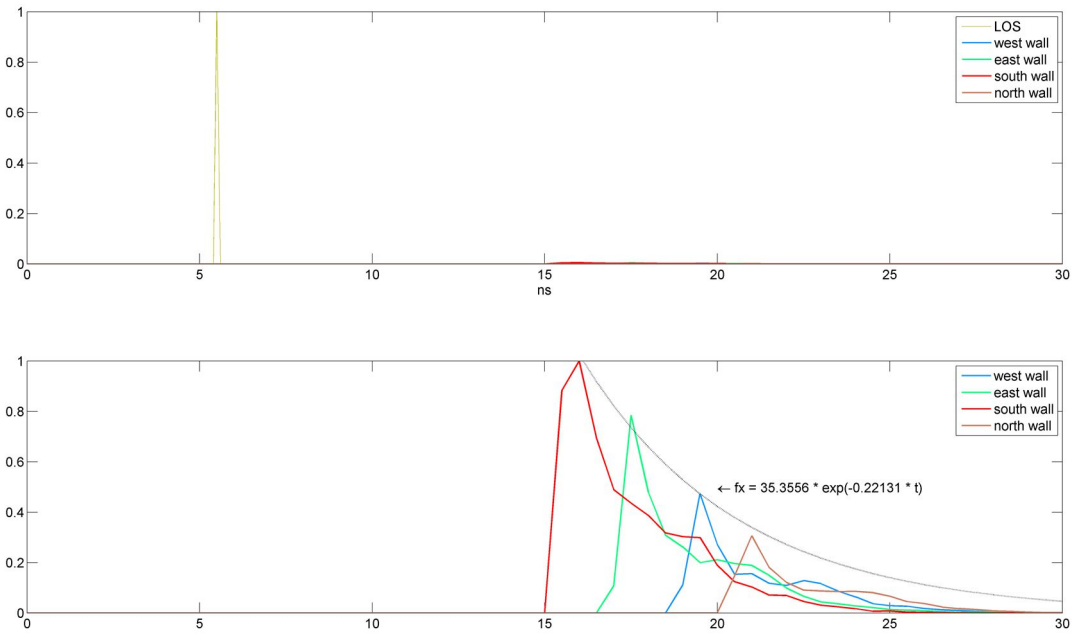


*Figure 25 – Propagation delay simulation 4.2, obstacle [0.4 ; -0.8; -1] , Room size 5x5x3*

Table 5 – Exponential distribution for reflected signal strength loss, describes exponential function determined from the peak value of each wall reflection for simulation 4.2. To determine coefficient for exponential function the matlab tool curve fitting.

*Table 5 – Exponential distribution for reflected signal strength loss*

| Room size | Exponential function | Bandwidth requirements |
|---|---|---|
| 4x4x3 | $f_x$=41.9 * $e^{(-0.286*t)}$ | 83 MHz |
| 5x5x3 | $f_x$=35.356 * $e^{(-0.221*t)}$ | 66 MHz |

When we compare the frequency selective figures for different room size, we can see the position of the pulse in comparison to case with constant reflective index ρ is identical, only amplitude of signal is different, which is in agreement with the simulation for smaller room (Figure 22). Time resolution is 0.5 ns

So to treat the walls as frequency selective has no influence on propagation delay as only reflectivity index varies, this way only energy of signal changes, but the time delay remains untouched.

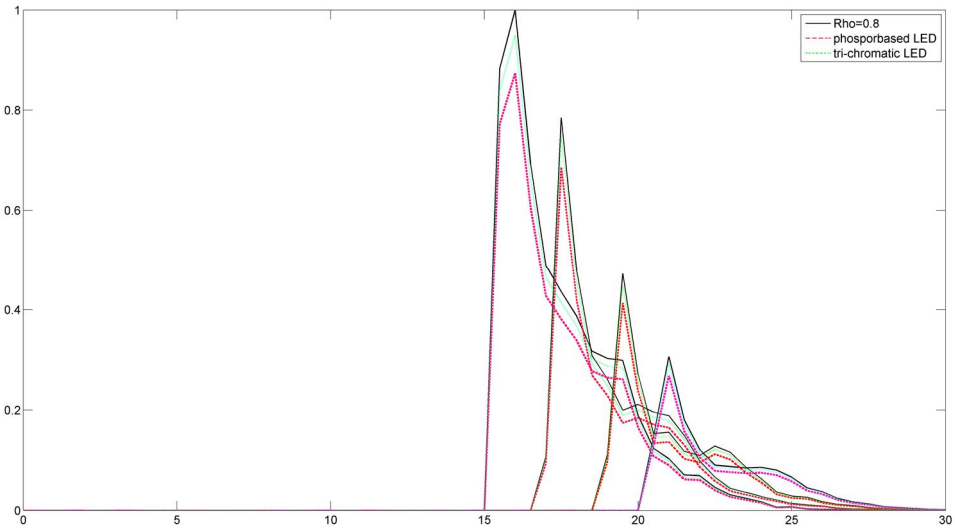


*Figure 26 - Channel Impulse Response simulation 4.2 – freq. selective surface, Room size 5x5x3*

## 4.3 Corridor

The Corridor can be characterized in that one room dimension is considerable larger than the other. The room (Corridor) paramters are shown in Table 6. Since the corridor is in one dimension significantly larger than rooms in previous simulations, situation with one and two transmitters is simulated.

*Table 6 - parameters for simulation 4.3*

| | |
|---|---|
| Room size 1st simulation | 2m x 10m x 3m |
| Detector area | 0.01 $m^2$ |
| Transmitted power by LED - $P_{per\ LED}$ | 0.01 W |
| Number of LED | 100 |
| Reflection coefficient ρ | 0.8 |
| Transmitter position [x,y,z]<br>2 x Transmitter positions [x,y,z] | 0 x 0 x 3m (on the ceiling)<br>-2 x 0 x 3m (on the ceiling)<br>+2 x 0 x 3m (on the ceiling) |
| Receiver height | 1 m |
| Semi-angle at half power $\theta$ | 70° |
| FOV of the receiver | 90° |

At first the received power with human in randomly chosen position is calculated, when only one source is present. Then, as depicted in Figure 27, scenario with two sources placed in appropriate position is simulated. The obstruction is represent by white rectangle.

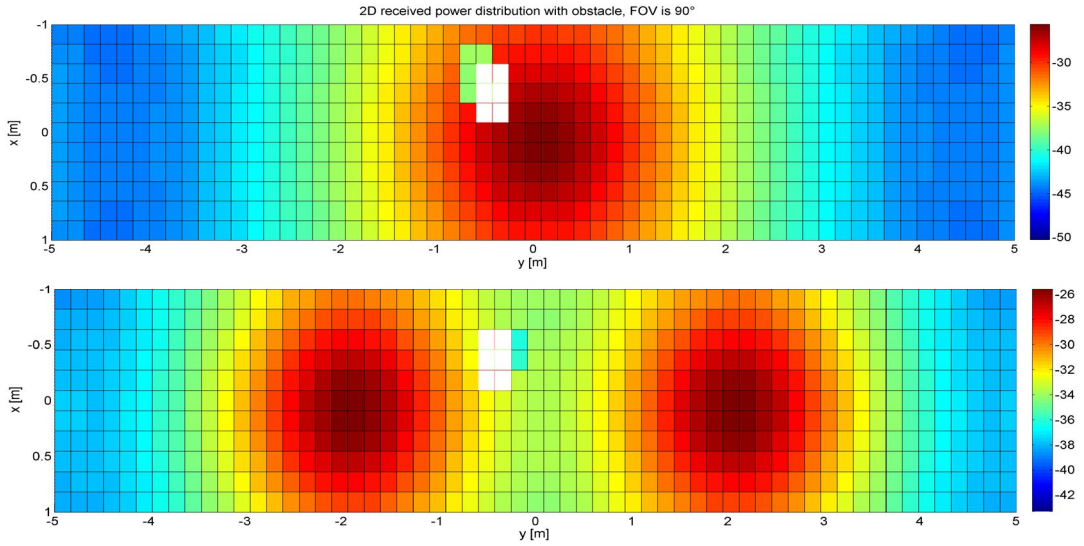


*Figure 27 - Received power distribution simulation 4.3 obstacle [-0.5 ; -0.5; -1.5]*

One source is not able to provide as much power, as two transmitters. Based on $\theta_{LED}$ and the receiver height it is possible there will be only NLOS link. In this case, this is not a problem, but it is appropriate give a notice. In the bottom subplot is visible that signal is stronger in the most part of corridor. If the receiver (human) is positioned between the transmitters, LOS link is available. From the power distribution point of view is second solution better.

But as mentioned in theoretical backround, the problem with non single source based systems is multipath propagation. Figure 28 shows the propagation delay for scenario with two sources. The thin line represents the reflected signal from the left source (position [0; -2 ; 3]), the rough line represents reflected signal from the source on the right, LOS component of link comes from source placed at [0; 2; 3] as well.

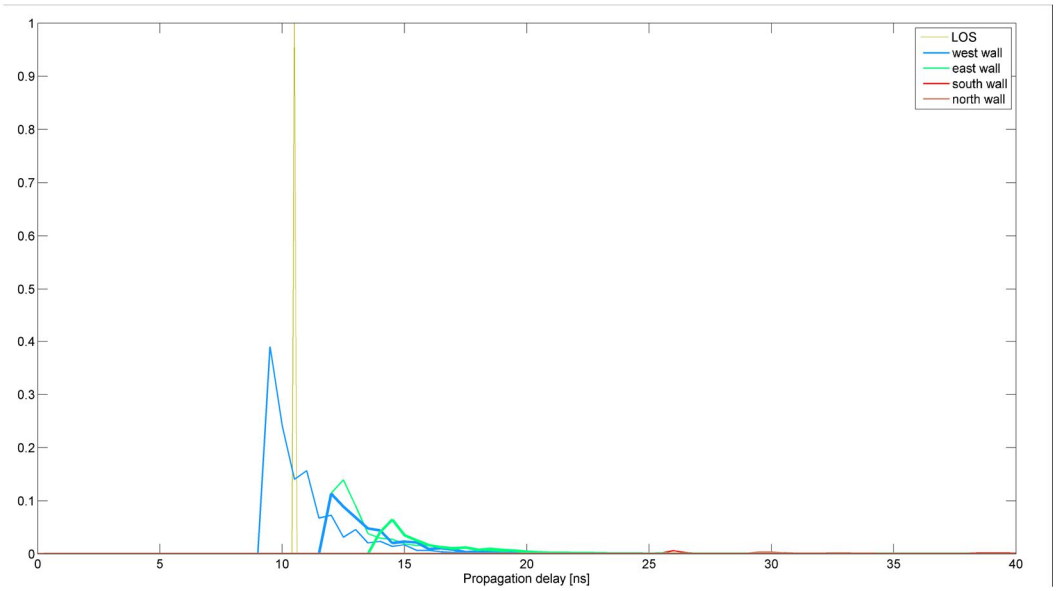


*Figure 28 – Propagation delay → simulation 4.3 obstacle [-0.5; -0.5; -1.5]*

As apparent LOS signal needs more time to reach the photodiode than reflected signal from the source on the left. Reflections from south and north walls (y coordinate -5/+5) is considerably attenuated.

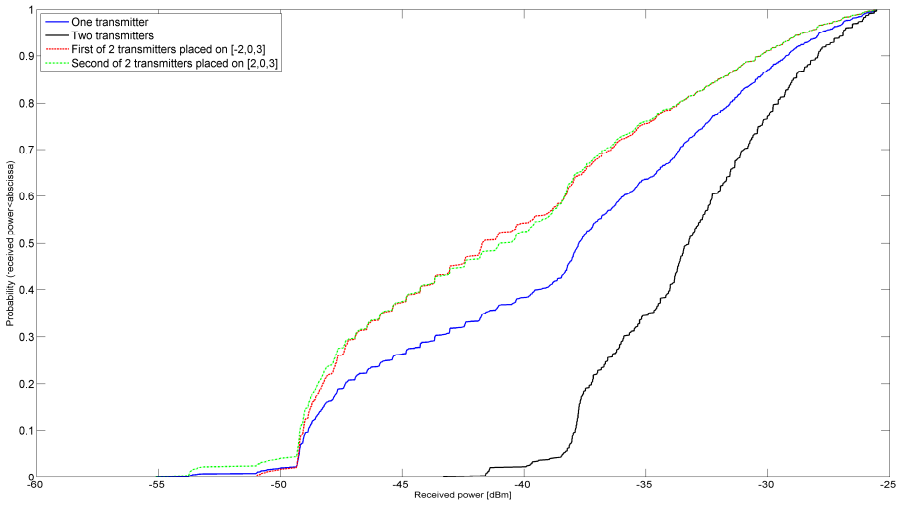


*Figure 29 - CDF for simulation 4.3 with one source and 2 sources*

Figure 29 shows CDF of received power. Received power in the 2-source based system from the individual receiver is weaker due to not optimal placement (from single-source based system point of view), but together they improve signal reception in the entire room so in this case in the Corridor.

## 4.4 Movement simulation

In this chapter impact on channel due to human movement is studied. As described in 3.4, modelled body is moving around the room in predefined pattern. Receiver is always

in the shadowed area, thus NLOS situation is analysed. Paramaters for simulation 4.4 are shown in Table 7.

*Table 7 - parameters for simulation 4.4*

| | |
|---|---|
| Room size 1st simulation | 4m x 4m x 3m |
| Detector area | 0.01 $m^2$ |
| Transmitted power by LED - $P_{per\ LED}$ | 0.01 W |
| Number of LED | 100 |
| Reflection coefficient ρ | 0.8 |
| Transmitter position [x,y,z] a) | 0 x 0 x 3m (on the ceiling) |
| Receiver height | 1 m, 1.2 m, 1.4 m |
| Semi-angle at half power $\theta$ | 60°, 70°, 80° |
| FOV of the receiver | 70°, 80°, 90° |

Figure 30 shows movement in the righ bottom part of the room on the first subplot. Human can move across the area in 8 different directions, individual steps are outlined in the figure.

The RMS spread value is represented by color point in every step (simulation position). For better visualization bottom subplot shows RMS depend on simulation step. RMS is calculated by using (21). The case when the $\theta_{LED}$ is 70° is displayed.

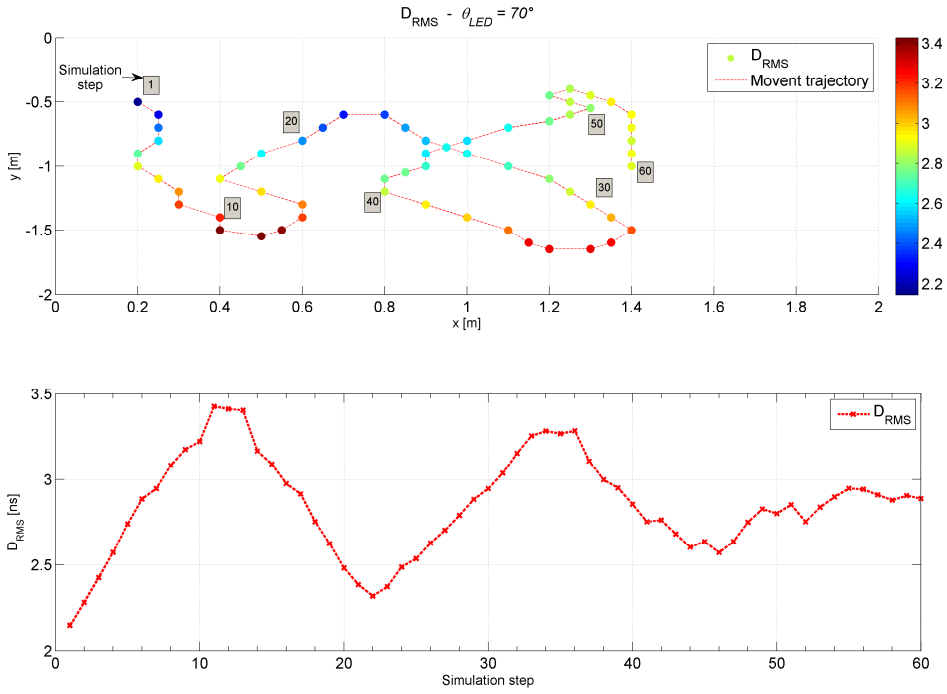


*Figure 30 - RMS delay spread*

Figure 31 has similar character as Figure 30. Top subplot shows mean delay spread in the room (x,y position) and the mean delay value represented by color point. Note that colorbar has the same color scale as the one in the figure above, but the range is different. Bottom subplot shows mean delay depend on simulation step. Mean delay is calculated by using (22). $\theta_{LED}$ is 70°, the closer to the wall the receiver is, the lower the mean delay is.

Figure 32 shows data speed (top subplot), received power (middle subplot) and RMS delay spread μ (bottom subplot) for every simulation step. Different $\theta_{LED}$ angles were simulated to determine impact of $\theta_{LED}$ to link parameters. Data speed is calculated by (23) and depends on RMS delay spread. Data speed is in Mbps.

With $\theta_{LED}$ increasing the available data speed decreases due to increased mean delay. Value of mean delay is higher with $\theta_{LED}$ increased. This is caused by reflection from the larger area as the higher $\theta_{LED}$ angle causes the optical power is radiated in more directions, this effects also total power received by the photodetector.

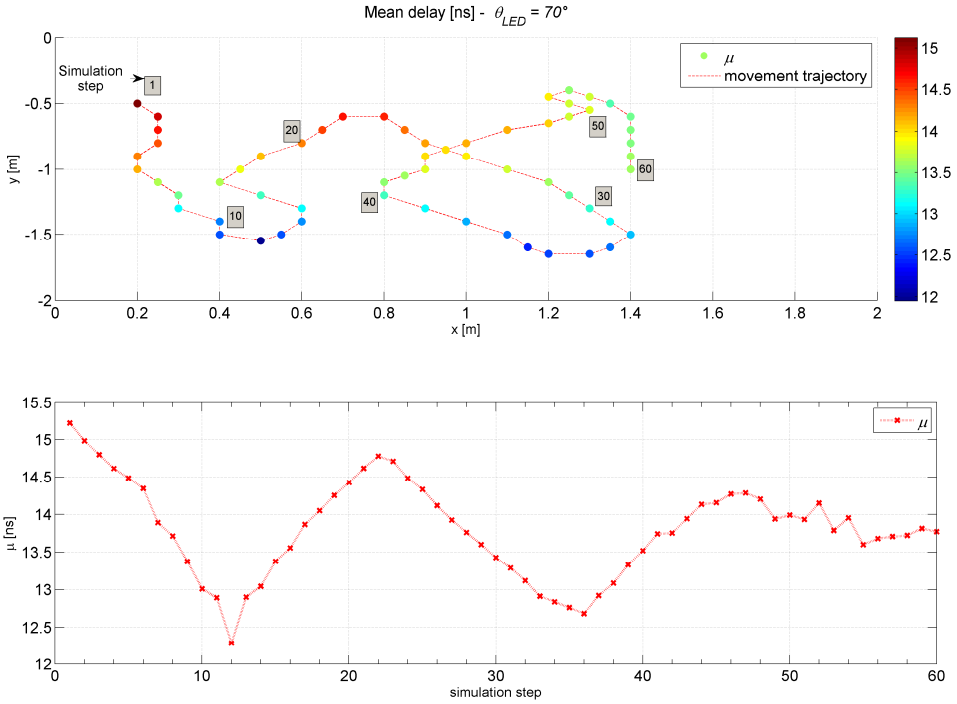


*Figure 31 - mean delay spread*

The more wall area reflects the optical energy, the more electrical energy can be converted from incident light. Note, that this is valid for NLOS link, in case of LOS link would be received power higher with $\theta_{LED}$ decreasing (because of Lambertian LED character).

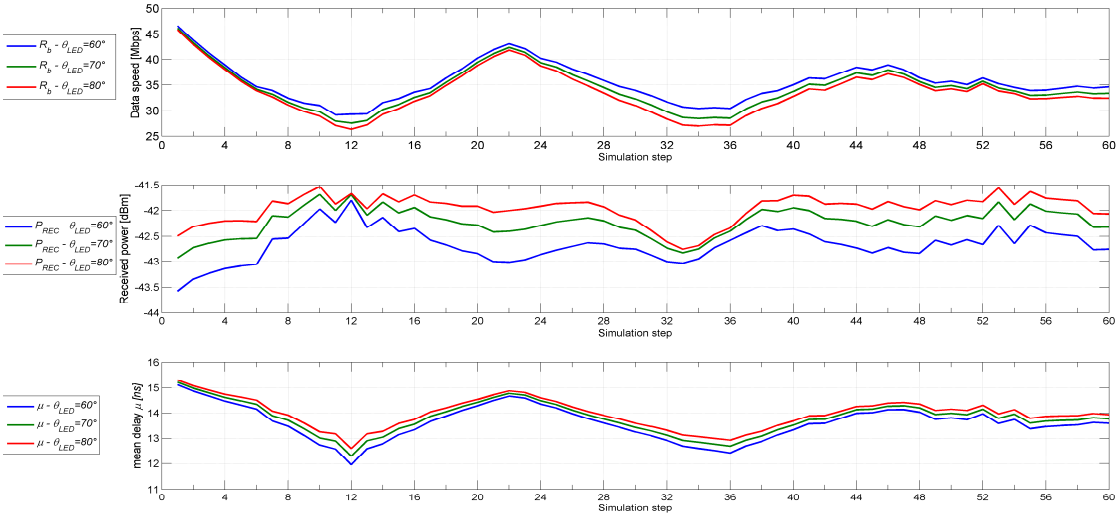


*Figure 32 - Transmission speed Rb, Received power Rc, mean delay*

Figure 33 shows how the mean spread value varies for different *FOV* receiver. For higher *FOV* raises the mean delay value. The higher the *FOV* angle is, the more reflected signal can the photodector receive, so the $\mu$ is higher.The mean delay $\mu$ was simulated for different $\theta_{LED}$ angles as well for the different photodector hight.

Receiver height 1m is displayed with a orange square marker, height 1.2m has marker of a blue triangle and the heighest receiver position is makred with inverted red triangle (triangle upside down). Corresponding $\theta_{LED}$ is shown in the righ figure side. We already found out that $\mu$ increases with the *FOV*. Simulation results also tells us heihger the receiver is, the smaller mean spread delay becomes, also inversely proportional effect to the $\mu$ value has increasing of $\theta_{LED}$ angle.

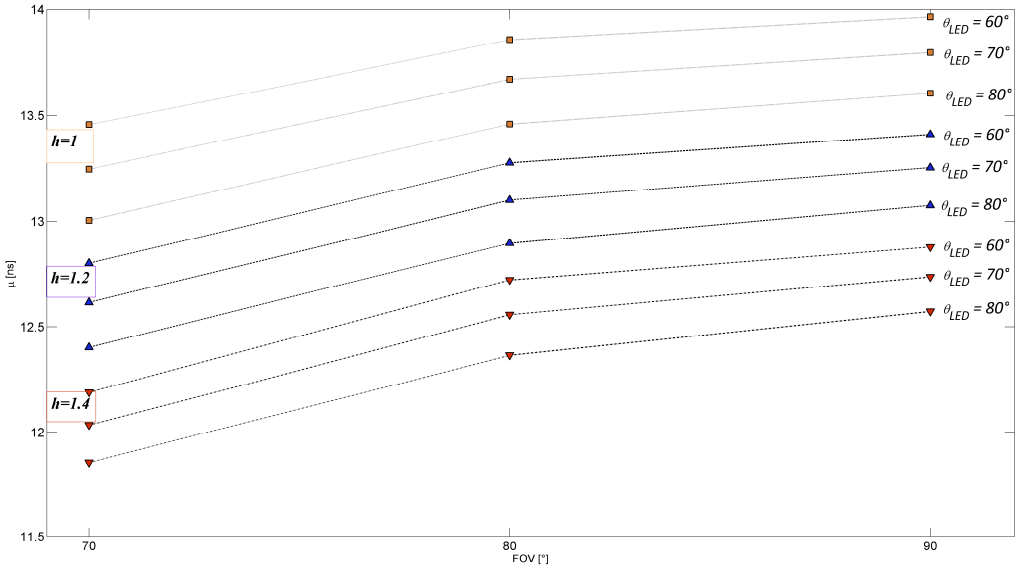


*Figure 33 - mean delay dependend on FOV / Receiver height*

The received power in the shaded area at photodetector is represented on Figure 34. Similar denotation as in the case above is used for this visualisation. Increased height of photodector lead to decrease in received power and the same effect has decreasing the receiver field of view → photodector is not able receive as much photons as in lower position or with higher *FOV*.

Increasing the source $\theta_{LED}$ leads to radiating into larger area, thus the more paths for the reflected signal are available and so the received power increases. Note that $\theta_{LED}$ is semi-angle at half power, sometimes refered to as $\theta_{½LED}$ .

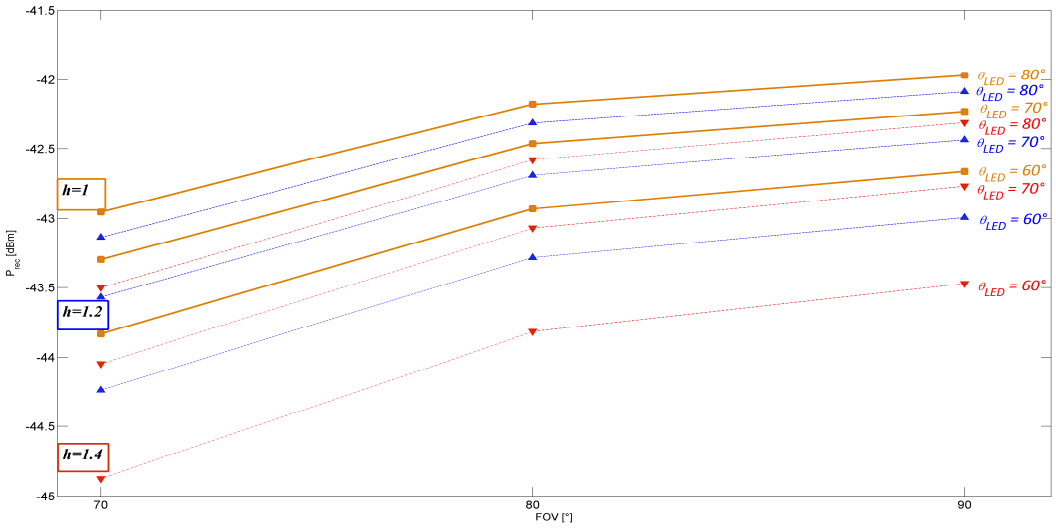


*Figure 34 - Received power dependend on FOV / Receiver height*

## 4.5 Summary

Simulation for the communication between devices (so-called device to device communication) is provided in 4.1. Decrease of received power in the simulation is in range from the ≈5dB to ≈11dB. Signal reflected from the wall opposite to the source showed to be relatively strong as in one case the reflected signal was ≈80% of the LOS link. Recevied power distribution is in range from ≈ -30dBm to ≈ -46dBm.

Next the scenario of the squared room with the source in the middle was modeled. Received power (under the similar conditions) is higher than in first case from ≈ -26 dBm to ≈ -40dBm. Drop in received power cause by shadowing is from ≈ -4dB to ≈ -8dB. Propagation delay shows more conventional situation and the reflected signal decreases, following exponential distribution displayed in Table 5 – Exponential distribution for reflected signal strength loss.

Increased room dimension causes ≈ 2dB decrease in received power in the majority of the room as visible from Figure 24. Reflection from modelled frequency selective wall cause less than 10% signal attenuation.

Corridor results shows that two transitters will enhance the received signal up to ≈ 10dB. Total range of received power by photodector is enhanced from ≈(-50dBm → -27dBm) in case of single-transmitter to ≈ (-42dBm → -26 dBm) for the system with 2 transmitters. Mean delay $\mu$ will increase from the 4.47ns to 9.98ns (in the receiver position) by adding second optical source.

RMS delay spread parameter of NLOS link cause by moving person varies in range from ≈2.1ns to ≈3.4ns for the receiver height 1m and $\theta_{LED}$ = 70°. Data link speed calculated from the (24) and is in range from 25 Mbps to 45Mbps. Meand delay is for FOV=70° ≈11.7ns to ≈13.5ns, for the FOV=80° $\mu$ is from ≈12.3ns to ≈13.8ns and for the FOV 90° the $\mu$ is in range from ≈12.5ns to ≈14ns.

Received power at the photodetector is for FOV from ≈ -44.8dBm to ≈ -43dBm. When the photodector FOV was 80° the received power is in range from ≈-44dBm to ≈-42.2dBm. For the full 90° field of view it Prec from ≈-43.5dBm up to ≈-42dBm.

# 5 CONCLUSION

In this diploma thesis, the different VLC scenario were investigated. The theoretical backround provided in the in the theoretical part offered the basis for simulation. The situation for the device to device communication showed the reflected signal can be considerable in some cases where the receiver is close to the opposite wall, which can affect the data speed, but on the other hand provides more robust system, thus offering better mobility.

More conventional scene was taken look into second simulation, where the transimitter is facing down and is placed in the middle of the room on the ceiling. In comparison with first simulation, the power distribution is better and object can cause less area with blocked LOS signal. The received signal in the shadowed area is stronger by several decibels. Loss of signal strength reflected from each wall can be descriebed with exponential function. This type of VLC link provides even better mobility.

After considering wall as frequency (wavelength) non-selective, the simulation of frequency selective has been provided. As expected, the frequency selective material does not change the received pulse position (in time), but it can change its amplitude.

In this case two different types of LED were simulated, both resulted in a bit higher decrease in received signal, but overall the difference was not significant and the use of identical ρ coefficient for all wavelengths proved to be appropriate. Cumulative distribution function were used to compare signal strength margin for room with larger size. To enhance the received signal it could be worth considering increasing the photodetector area from 1cm2 (for example. 1cm x 1cm) to 10cm2 (2.5cm x 4cm or 3.3cm x 3.3 cm) to gain 10dB.

Corridor scenario, where the one one dimension is dominant, shows that the energy from one transmitter does not have to be enough, so the possibility rely on double-transmitter based system is available. Simulation proved that power distribution will improve, but at cost of delay propagation increase. Cumulative distribution function is provided to better visualize the difference between single-source based VLC system and the case with 2 sources.

The last considered scenario is similar to second simulation with the transmitter in the middle of the room, but the movement of person is added into the simulation. Results indicates that achievable in NLOS link is from 25Mbps to 45Mbps, with received power from –45dBm to -42dBm for all simulated scenario, thus mobility is not a problem in VLC systems.

# 6 REFERENCE


[1] DIMITROV, S., HARALD, H., : *Principles of LED light communications: towards networked Li-Fi*. United Kingdom: TJ International Ltd. Padstow Cornwall, 2015, p. 12-31. ISBN 9781107049420.

[2] GHASSEMLOOY, Z., POPOOLA, W., RAJBHANDARI, S., *Optical wireless communications: system and channel modelling with MATLAB*. Boca Raton, FL: Taylor & Francis, 2012. ISBN 9781439851883.

[3] *Design of an Optical Pulse Position Modulation (O-PPM) Direct Translating Receiver* [online]. [q. 2016-11-10]. Available : http://csi.usc.edu/csi30/35.pdf

[4] ALDIBBIAT, N.M., GHASSEMLOOY Z., MCLAUGHLIN R., : *Dual header pulse interval modulation for dispersive indoor optical wireless communication systems*. IEEE Proceedings - Circuits, Devices and Systems. 2002, 149(3), 187-192. DOI: 10.1049/ip-cds:20020422. ISSN 1350-2409. Available: http://digital-library.theiet.org/content/journals/10.1049/ip-cds_20020422

[5] Jing Ch., Yong A., Ying T.,: *Improved free space optical communications performance by using time diversity*. Chin. Opt. Lett. 6, 797-799 (2008) available: https://www.osapublishing.org/col/abstract.cfm?URI=col-6-11-797

[6] COLEMAN, D.,: *CWNA certified wireless network administrator official study guide*. Third Edition. Indianapolis, Indiana: John Wiley, 2012. ISBN 11-181-2779-X.

[7] *What Wavelength Goes With a Color*. [online]. [2016-11-23]. Available: https://science-edu.larc.nasa.gov/EDDOCS/Wavelengths_for_Colors.html

[8] ELGALA, H., MESLEH R., HAAS H., : *OFDM Visible Light Wireless Communication Based on White LEDs*. 2007 IEEE 65th Vehicular Technology Conference - VTC2007-Spring [online]. IEEE, 2007, p. 2185-2189 [ 2016-11-12]. DOI: 10.1109/VETECS.2007.451. ISBN 1-4244-0266-2. ISSN 1550-2252. Available: http://ieeexplore.ieee.org/document/4212879/

[9] KOMINE, T., NAKAGAWA, M.,: *Fundamental analysis for visible-light communication system using LED lights*. IEEE Transactions on Consumer Electronics. 2004, 50(1), 100-107. DOI: 10.1109/TCE.2004.1277847. ISSN 0098-3063. Available: http://ieeexplore.ieee.org/document/1277847/

[10] LOURO, P., SILVA V., COSTA J., VIEIRA M.,: *Transmission of Signals Using White LEDs for VLC Application*. MRS Advances. ,p. 1-6. DOI: 10.1557/adv.2016.372. ISSN 2059-8521. Available: http://www.journals.cambridge.org/abstract_S2059852116003728

[11] LEE, K., Hyuncheol, P., BARRY, R.,: *Indoor Channel Characteristics for Visible Light Communications*. IEEE Communications Letters. 2011, 15(2), 217-219. DOI:

10.1109/LCOMM.2011.010411.101945. ISSN 1089-7798. Available: http://ieeexplore.ieee.org/document/5682214/

[12] Chung, G., : *Visible Light Communication, Advanced Trends in Wireless Communications*, Dr. Mutamed Khatib (Ed.), ISBN: 978-953-307-183-1, InTech, Available: http://www.intechopen.com/books/advanced-trends-in-wireless-communications/visible-light-communication

[13] KIKUCHI, K.,: *High spectral density optical communication technologies*. New York: Springer, c2010, p. 11-49. Optical and fiber communications reports, 6. ISBN 3642104193.

[14] GAGLIARDI, R., Sherman. K.,: *Optical communications*. 2nd ed. New York: Wiley, c1995. ISBN 04-715-4287-3.

[15] RYU, S.,: *Coherent Optical Communication Systems*. Boston: Artech House, c1995. ISBN 08-900-6612-4.

[16] RAJAGOPAL, S., ROBERTS, R., Sang-Kyu L., : *IEEE 802.15.7 visible light communication: modulation schemes and dimming support*. IEEE Communications Magazine. 2012, 50(3), 72-82. DOI: 10.1109/MCOM.2012.6163585. ISSN 0163-6804. Available: http://ieeexplore.ieee.org/document/6163585/

[17] Chi-Wai, C., I-Cheng, L., Yen-Liang, L., Chien-Hung, Y.,: *High Speed Imaging 3 × 3 MIMO Phosphor White-Light LED Based Visible Light Communication System*. IEEE Photonics Journal. 2016, 8(6), 1-6. DOI: 10.1109/JPHOT.2016.2633395. ISSN 1943-0655. Available: http://ieeexplore.ieee.org/document/7776773/

[18] CZAPUTA, M., JAVORNIK, T., LEITGEB, E., KANDUS, G.,: ConTEL 2011: *proceedings of the 11th International Conference on Telecommunications,* June 15-17, 2011, Graz, Austria [online]. Zagreb: University of Zagreb, Faculty of Electrical Engineering and Computing, 2011, p. 359-362 [q. 2016-12-15]. ISBN 9783851251616.

[19] ZENG, L., O'BRIEN, D., MINH, H., FAULKNER, G., LEE, K.,: *High data rate multiple input multiple output (MIMO) optical wireless communications using white led lighting*. IEEE Journal on Selected Areas in Communications. 2009, 27(9), 1654-1662. DOI: 10.1109/JSAC.2009.091215. ISSN 0733-8716. Available: http://ieeexplore.ieee.org/document/5342325/

[20] ZIXIONG, W.,, WEN-DE, Z., SONGNIAN, F., : *Performance comparison of different modulation formats over free-space optical (FSO) turbulence links with space diversity reception technique*. IEEE Photonics Journal. 2009, 1(6), 277-285. DOI: 10.1109/JPHOT.2009.2039015. ISSN 1943-0655. Available: http://ieeexplore.ieee.org/document/5357442/

[21] BO, B., ZHENGYUAN, X., YANGYU, F.,: *Joint LED dimming and high capacity visible light communication by overlapping PPM*. The 19th Annual Wireless and Optical Communications Conference (WOCC 2010). IEEE, 2010, 2010(19th), 1-5. DOI: 10.1109/WOCC.2010.5510410. ISBN 978-1-4244-7597-1. Available: http://ieeexplore.ieee.org/document/5510410/

[22] KATO, K., HATA, S., KOZEN, A., *High-efficiency waveguide InGaAs pin photodiode with bandwidth of over 40 GHz*. IEEE Photonics Technology Letters. 1991, 3(5), 473-474. DOI: 10.1109/68.93883. ISSN 1041-1135. Available: http://ieeexplore.ieee.org/document/93883/
[23] James, B.,: *NATO Science for Peace and Security Series B: Physics and Biophysics: Originally published with the title: NATO Security through Science Series B*: Physics and Biophysics. Dordrecht, Netherlands: Springer, 2009, 20 July–2 August 2008(1st). ISSN 1874-6500.
[24] ETTENBERG, M., KRESSEL, H., WITTKE, J.,: *Very high radiance edge-emitting LED*. IEEE Journal of Quantum Electronics. 1976, 12(6), 360-364. DOI: 10.1109/JQE.1976.1069158. ISSN 0018-9197. Available : http://ieeexplore.ieee.org/document/1069158/
[25] John, M., Yousif, M.,. *Optical fiber communications: principles and practice*. 3rd ed. New York: Financial Times/Prentice Hall, 2009. ISBN 01-303-2681-X.
[26] Refractive index database. Refractive index database: RefractiveIndex.INFO website [online]. 2016 [quoted. 2016-12-01]. Available: http://refractiveindex.info/?shelf=organic&book=methane&page=Martonchik-liquid-111K